UNIVERSIDADE DE LISBOA
FACULDADE DE CIÊNCIAS
DEPARTAMENTO DE BIOLOGIA VEGETAL

Long non-coding RNAs as potential therapeutic targets in human breast cancer

Ana Beatriz Domingues Silva

Mestrado em Biologia Molecular e Genética

Dissertação orientada por:
Doutor Bruno Miguel Bernardes de Jesus
Doutora Maria Helena Caria

2018

Agradecimentos

Em primeiro lugar quero agradecer à Professora Doutora Helena Caria por me ter proporcionado a primeira aventura num laboratório, por estar sempre disponível para mim e pela revisão desta dissertação. Em segundo lugar quero agradecer à Doutora Carla Gomes e ao Doutor Bruno de Jesus por me terem aceite como aluna de mestrado para realizar este projeto. Sempre quis tralhar na área do cancro portanto foi uma ótima oportunidade para mim. Quero também agradecer por todo o apoio prestado no planeamento/execução experimental e na revisão desta dissertação. Em terceiro lugar, quero agradecer à Catarina do Vale por ter sido a principal impulsionadora deste projeto e pela ajuda na realização de algumas experiências. Ao Sérgio Marinho quero agradecer por me ensinar algumas técnicas laboratoriais e por me esclarecer as dúvidas sempre que surgiam. À Dinora quero agradecer pela ajuda na realização das encomendas. Aos meus colegas de laboratório quero agradecer pela boa-disposição, animação e companhia. À unidade de bioimagem, principalmente ao António Temudo, quero agradecer pelo apoio na visualização e aquisição de imagens de microscopia de fluorescência. À unidade de citometria de fluxo quero agradecer pelo apoio na realização e análise dos resultados de apoptose e ciclo celular.

Muito obrigado à minha família em geral por ter feito de mim aquilo que sou hoje e por ser o meu porto de abrigo. Muito obrigado, em particular, aos meus pais, Emídio da Silva e Ana Maria Silva, e aos meus irmãos, Jorge Silva e João Silva, por serem os melhores do mundo e os principais responsáveis por eu estar hoje a terminar a minha tese de mestrado, por me proporcionarem todas as condições, pelos conselhos, palavras de incentivo e conforto em momentos mais difíceis, pelo carinho e amor incondicionais. Um obrigado especial ao meu namorado, Bernardo Antunes, pela paciência, por ouvir as minhas frustrações e euforias, pelos momentos de descontração após longos dias de trabalho, pela amizade e pelo amor. Percorremos este caminho juntos e isso tornou tudo muito mais fácil. Por fim, obrigada às minhas melhores amigas, Rita Rodrigues e Sara Castro, que ao fim de tantos anos continuam a estar presentes tanto nos bons como nos maus momentos.

Abstract

Long non-coding RNAs have emerged as regulators of diverse biological processes but little is known about their role in cancer. The recently discovered human lncRNA NORAD is induced after DNA damage in a p53-dependent manner and plays a critical role in the maintenance of genomic stability, since interacts with Pumilio proteins, limiting the repression of their target mRNAs involved in mitosis, DNA repair and replication. Therefore, NORAD inactivation causes chromosomal instability and aneuploidy, which contributes to accumulation of genetic abnormalities and tumorigenesis. However, severe chromosome mis-segregations end up with cell death, suggesting that NORAD may act as an oncogene and tumor suppressor gene. Moreover, this lncRNA has been detected in several types of cancer, including breast cancer, which is the most frequently diagnosed and the second-leading cause of cancer death in women. However, some studies present contradictory results relative to NORAD function in tumorigenesis.

In the present study was found that NORAD expression is upregulated in a set of human epithelial breast cancer cell lines (MDA-MB-231, 436 and 468), which belong to the most aggressive triple negative subtype, in comparison to a non-malignant human mammary epithelial cell line (MCF-10A) by RT-qPCR. In agreement, was found that high NORAD expression levels in basal-like tumors are associated with poor prognosis, through Kaplan-Meier Plotter tool. In order to unravel the role of this lncRNA, tumor-relevant phenotypes were analyzed after its knockdown, using LNA™ GapmeRs and siRNAs, in the MDA-MB-231 cell line. Cell proliferation inhibition determined by alamarBlue® reduction assay and cell migration inhibition determined by wound healing assay, suggests that NORAD acts as an oncogene. In addition, upon NORAD knockdown, was identified a shift in doxorubicin IC_{50} from 0.3779 μM to 0.05680 μM by alamarBlue® reduction assay caused by an increase in cell death, indicating sensitization to chemotherapy. In fact, chromosomal instability generated upon NORAD knockdown, in combination with DNA damage induced by doxorubicin results in severe chromosome mis-segregations, incompatible with cell viability. In contrast, no cell cycle change was identified by flow cytometry because this lncRNA is not required for these aspects of the DNA damage response. This study also highlights the role of p53, guardian of the genome, in the response to these stress conditions, since its expression levels increase (RT-qPCR and western blot), inducing cell cycle arrest or apoptosis.

These results provide evidences that the lncRNA NORAD represents a tumor marker for disease diagnosis, patient prognosis or therapy response, and represents a therapeutic target in breast cancer.

Keywords: breast cancer, DNA damage, p53, NORAD, chromosomal instability

Resumo

O projeto ENCODE (Enciclopédia de Elementos do DNA) estima que apenas 2% do genoma humano codifica proteínas, enquanto 75% é transcrito em RNAs não codificantes de pequenas e de grandes dimensões. Cerca de 16.000 genes codificam mais de 28.000 RNAs longos não codificantes (lncRNAs), os quais têm sido alvo de interesse por participarem em diferentes processos biológicos (desenvolvimento, doenças, etc.). Geralmente, os lncRNAs são constituídos por mais de 200 nucleótidos, pouco conservados evolutivamente, pouco abundantes e heterogéneos. Recentemente foi descoberto um transcrito com 5,3 kb (*LINC00657*) que se destaca por ser muito conservado evolutivamente, muito abundante e constitutivamente expresso. Localiza-se predominantemente no citoplasma onde pode regular a estabilidade e tradução de RNAs mensageiros (mRNAs) e influenciar a sinalização celular. No núcleo pode organizar a estrutura subnuclear, regular a transcrição e interações cromossómicas. Após danos no DNA, este lncRNA é ativado de modo dependente de p53, sendo por isso denominado NORAD (RNA não codificante ativado por danos no DNA). NORAD, que contém 17 regiões de reconhecimento de proteínas de ligação ao RNA designadas Pumilio (sequência específica: UGUANAUA), captura uma quantidade significativa destas proteínas, impedindo que inibam a tradução de mRNAs alvo com os quais interagem através da sua região 3', onde se encontra a sequência específica. Esses transcritos atuam ao nível da homeostasia da linha germinal, atividade neuronal, mitose, replicação e reparação do DNA. É importante referir que a interação entre o lncRNA NORAD e as proteínas Pumilio é induzida por outra proteína de ligação ao RNA, SAM68, que se liga a jusante das regiões de reconhecimento das proteínas Pumilio. Assim, na ausência de NORAD, as proteínas Pumilio são ativadas e inibem a tradução de mRNAs alvo, o que perturba a segregação dos cromossomas durante a mitose e provoca aneuploidia. Por sua vez, a aneuploidia pode contribuir para o ganho de funções por parte de oncogenes e a perda de funções por parte de genes supressores de tumores, originando tumores. Neste caso, NORAD atua como um gene supressor de tumores. Contudo, quando a acumulação de erros durante a mitose se torna demasiado elevada, as células não têm capacidade de resposta e morrem. Neste caso, NORAD atua como um oncogene. Estudos demonstraram a expressão de NORAD em vários tipos de cancro, no entanto, alguns resultados são contraditórios no que respeita à sua função. Nas células e tecidos dos cancros da mama, do esófago e do pâncreas detetaram-se níveis de expressão mais elevados em comparação com as respetivas células e tecidos normais, bem como uma correlação entre os seus níveis e o pior prognóstico dos pacientes. Além disso, depois da redução da expressão de NORAD, analisaram-se os efeitos nas propriedades das células e verificou-se redução da viabilidade, proliferação, migração e invasão *in vitro* e *in vivo*. Pelo contrário, nas células e tecidos do cancro do fígado detetaram-se níveis de expressão mais baixos em comparação com as respetivas células e tecidos normais, bem como uma correlação entre os seus níveis e o melhor prognóstico dos pacientes. Além disso, depois da redução da expressão de NORAD, analisaram-se os efeitos nas propriedades das células e verificou-se aumento da proliferação, ciclo celular, migração e invasão *in vitro* e *in vivo*.

O presente estudo centra-se no cancro da mama por ser o mais frequentemente diagnosticado e o segundo mais mortífero em mulheres. É também uma doença complexa pois apresenta diferentes subtipos (luminal, HER2 positivo e basal) definidos de acordo com a presença de três recetores (ER, PR e HER2) e que apresentam diferentes características morfológicas e genéticas, resultando em diferentes tratamentos e prognósticos. Em primeiro lugar, determinaram-se os níveis basais de expressão de NORAD em células de cancro da mama (MCF-7, MDA-MB-231, 468 e 436) em comparação com células normais (MCF-10A) por RT-qPCR, tendo sido registados níveis de expressão mais elevados nas células de cancro da mama mais agressivas, isto é, negativas para os três recetores (MDA-MB-231, 468 e 436). A predominante localização citoplasmática deste lncRNA foi confirmada por smRNA FISH. Em segundo lugar, efetuou-se a redução da expressão de NORAD usando LNA™ GapmeRs que atuam essencialmente ao nível do núcleo e siRNAs que atuam essencialmente ao nível do citoplasma. O

resultado foi confirmado por RT-qPCR e por smRNA FISH. Em terceiro lugar, analisaram-se os efeitos da redução da expressão de NORAD nas propriedades tumorais da linha celular MDA-MB-231, e verificou-se inibição da proliferação através do ensaio da redução de alamarBlue® e inibição da migração através do ensaio de migração *in vitro*. A capacidade de proliferação e de metastização são características fundamentais do cancro, logo, estes resultados indicam que este lncRNA desempenha um papel importante na tumorigénese. De seguida, avaliou-se o efeito da combinação da redução da expressão de NORAD com quimioterapia. Para isso, utilizou-se a doxorrubicina que pertence à classe das antraciclinas, intercala-se entre pares de bases no DNA e inibe a topoisomerase II, provocando danos no DNA. Nestas condições, identificou-se uma redução do IC_{50} da doxorrubicina de 0,3779 μM para 0,05680 μM através do ensaio da redução de alamarBlue®, o que sugere que a redução da expressão de NORAD sensibiliza as células do cancro da mama à quimioterapia. Isto assume principal relevância em casos de resistência à quimioterapia. De acordo com este resultado, nas mesmas condições verificou-se um aumento da apoptose celular através de citometria de fluxo. De facto, a instabilidade cromossómica originada pela redução da expressão de NORAD e os danos no DNA originados pela doxorrubicina, levam à acumulação de demasiados erros genéticos que resultam na morte celular. Por outro lado, não se registaram alterações no ciclo celular para além da acumulação das células na fase G_2 induzida pela doxorrubicina, porque este lncRNA não participa nesse tipo de resposta aos danos no DNA. No presente estudo é ainda destacado o gene supressor de tumores p53 como o guardião do genoma por ser ativado em condições de stress, ligar-se a proteínas envolvidas na reparação do DNA (XPB, RPA e rad51) e promover a transcrição de p21 que inibe cinases dependentes de ciclinas que regulam as transições G_1-S e G_2-M, induzindo arrastamento do ciclo celular. Em alternativa, quando os danos no DNA são demasiado elevados, ocorre apoptose celular através da libertação do citocromo c, da expressão de proteínas pro-apoptóticas da família BCL-2 (por exemplo, *puma*, *noxa*, *bid* e *bax*), de componentes da sinalização do recetor de morte celular (por exemplo, DR5 e Fas/CD95) ou da maquinaria efetora de morte celular (por exemplo, caspase-6, Apaf-1 e PIDD). De facto, perante a instabilidade cromossómica gerada pela redução da expressão de NORAD e os danos no DNA gerados pela doxorrubicina, detetou-se um aumento da expressão de p53 por RT-qPCR e western blot. Por fim, recorreu-se ao teste de Kaplan Meier para avaliar o efeito da expressão de NORAD na sobrevivência de pacientes com cancro da mama. Apenas para o subtipo basal que é o mais agressivo, se verificou uma correlação entre níveis de expressão de NORAD elevados e menor tempo de sobrevivência livre de recidiva.

Os resultados obtidos permitem inferir que o lncRNA NORAD pode representar um biomarcador importante para o diagnóstico de cancro, o prognóstico do paciente e a resposta a terapias, e pode representar um alvo terapêutico. No futuro, aumentar a expressão de NORAD em células da mama normais (MCF-10A) e avaliar se existe aquisição de fenótipo tumoral, seria uma boa estratégia para esclarecer se este lncRNA é fundamental na tumorigénese.

Palavras-chave: cancro da mama, danos no DNA, p53, NORAD, instabilidade cromossómica

Index

List of figures, tables and equations

List of abbreviations

RAS – rat sarcoma gene
TP53 – tumor protein p53
BRCA 1/2 – breast cancer susceptibility 1/2 gene
RB1 – retinoblastoma 1 gene
ER – estrogen receptor
PR – progesterone receptor
HER2 – human epidermal growth factor receptor 2
PARP – poly (ADP-ribose) polymerase
Mdm2 – murine double minute 2 gene
ARF – ADP-ribosylation factor
CDK – cyclin-dependent kinase
BCL-2 – B-cell lymphoma 2 gene
Puma – p53 upregulated modulator of apoptosis
Bid – BH3 interacting domain death agonist
Bax – Bcl-2-associated X protein
oxLDL – oxidized low-density lipoprotein
HIF-1α – hypoxia-inducible factor 1α
VEGF – vascular endothelial growth factor
MMP – matrix metalloproteinase
PCA3 – prostate cancer associated 3
PCGEM1 – prostate-specific transcript 1
CREB3L1 – cAMP response element-binding protein 3-like 1
PTEN – phosphatase and tensin homolog
ATM – ataxia telangiectasia mutated
MDC1 – mediator of DNA damage checkpoint 1
Mre11 – meiotic recombination 11 homolog
Nbs1 – Nijmegen breakage syndrome 1 gene
53BP1 – TP53-binding protein 1
PP2A – protein phosphatase 2A
RNF 2/8/168 – ring finger protein 2/8/168
BMI1 – B lymphoma Mo-MLV insertion region 1 homolog
HCC – hepatocellular carcinoma
TNM – tumor, node and metastasis
UICC – Union for International Cancer Control
OS – overall survival
RFS – relapse-free survival
sncRNA – short non-coding RNA
lncRNA – long non-coding RNA
NORAD – non-coding RNA activated by DNA damage
PRE – PUMILIO recognition element
PUM – Pumilio protein
PUF – Pumilio-Fem3-binding factor
RNP – ribonucleoprotein
ND – NORAD domain
CIN – chromosomal instability
RBP – RNA-binding protein

SAM68 – SRC associated in mitosis
ceRNA – competing endogenous RNA
ACTB – β-actin
RT-qPCR – real-time quantitative reverse transcriptase polymerase chain reaction
C_t – threshold cycle
smRNA FISH – single-molecule RNA fluorescence *in situ* hybridization
DAPI – 4', 6-diamidino-2-phenylindole
CRISPR-Cas9 – clustered regulatory interspaced short palindromic repeats-associated endonuclease 9
TALEN – transcription activator-like effector nucleases
RNAi – RNA interference
shRNA – short hairpin RNA
siRNA – small interfering RNA
LNA – locked nucleic acid
Scr – scramble
KD – knockdown
IC_{50} – half maximal inhibitory concentration
DMEM – Dulbecco's Modified Eagle Medium
FBS – fetal bovine serum
PBS – phosphate-buffered saline
PFA – paraformaldehyde
FA – formamide
SSC – saline sodium citrate
SDS-PAGE – sodium dodecyl sulfate-polyacrylamide gel electrophoresis
APS – ammonium persulfate
TEMED – tetramethylethylenediamine
HRP – horseradish peroxidase
BCA – bicinchoninic acid
FACS – fluorescence activated cell sorting
7-AAD – 7-aminoactinomycin D
PS – phosphatidylserine
RT – room temperature

1. Introduction

1.1 Hallmarks of cancer

In 2000, Hanahan and Weinberg proposed six hallmarks of cancer, which are distinctive and complementary capabilities that enable tumor growth and metastatic dissemination: (1) sustaining proliferative signaling; (2) evading growth suppressors; (3) enabling replicative immortality; (4) activating invasion and metastasis; (5) inducing angiogenesis; and (6) resisting cell death (1).

Their acquisition is possible by two enabling characteristics. Most prominent is genomic instability, which consists in the accumulation of alterations in the genome, some that confer selective advantage on subclones of cells, enabling their outgrowth and eventual dominance in a local tissue environment (2). These alterations in the genome include gain-of-function mutations in oncogenes (e.g. *RAS*) (is sufficient to have a mutation in one of the two alleles) that normally stimulate cell growth, division and survival, and loss-of-function mutations in tumor suppressor genes (e.g. *TP53*) (is necessary to have a mutation in both alleles) that normally prevent unrestrained cellular growth, promote DNA repair and cell cycle checkpoints activation (3). This process can be accelerated by an increasing sensitivity to mutagenic agents, breaking down components of the genomic maintenance machinery, compromising surveillance systems that force genetically damaged cells into either senescence or apoptosis, and losing the telomeric DNA. Regarding the other enabling characteristic, some tumors are densely infiltrated by cells of the innate and adaptive immune system, which reflect an attempt of eradication or contribute to multiple hallmarks by supplying bioactive molecules to the tumor microenvironment, including growth factors that sustain proliferative signaling, survival factors that limit cell death, pro-angiogenic factors and extracellular matrix-modifying enzymes that facilitate angiogenesis and metastasis, and inductive signals of epithelial-mesenchymal transition and of other hallmark-facilitating programs. In addition, inflammatory cells can release chemicals, notably reactive oxygen species, that are actively mutagenic for nearby cancer cells (2).

Yet, other attributes of cancer cells have been proposed to be functionally important for the development of cancer: reprogramming of cellular energy metabolism and active evasion from attack and elimination by immune cells. Otto Warburg observed that even in the presence of oxygen, cancer cells can reprogram their glucose metabolism, almost limiting it to glycolysis. They compensate for the approximately 18-fold lower efficiency of ATP production in comparison to mitochondrial oxidative phosphorylation, by upregulating glucose transporters, notably GLUT1, which substantially increase glucose import into the cytoplasm (2,4). Of note, glycolytic intermediates participate in various biosynthetic pathways, including those generating nucleosides and amino acids, which facilitate the formation of macromolecules and organelles required for the assembly of new cells. Moreover, tissues are monitored by an ever-alert immune system, responsible for recognizing and eliminating the majority of incipient cancer cells. Therefore, solid tumors that do appear, disable components of the immune system such as cytotoxic T lymphocytes and natural killer cells, through secretion of TGF-β or other immunosuppressive factors, and recruit inflammatory cells that are actively immunosuppressive such as regulatory T cells and myeloid-derived suppressor cells (2).

1.2 Tumor microenvironment

Initially, tumors were thought of as a collection of relatively homogeneous cells, whose entire biology could be understood by elucidating the cell-autonomous properties. However, the recognition of the tumor complexity changed this perspective. In fact, the biology of a tumor can only be understood by studying the individual specialized cell types within it, as well as the tumor microenvironment that they construct during the course of multistep tumorigenesis. These are: cancer cells, cancer stem cells,

endothelial cells, pericytes, immune inflammatory cells, cancer-associated fibroblasts, stem and progenitor cells of the stroma. The likelihood that signaling interactions between cancer cells and their supporting stroma evolve during the course of multistep tumorigenesis, complicates the goal of fully elucidating the mechanisms of cancer pathogenesis. Therefore, understanding these dynamic variations is crucial to the development of novel therapies designed to successfully target both primary and metastatic tumors (2).

1.3 Breast cancer

Breast cancer is the most frequently diagnosed cancer and the second-leading cause of cancer death in women (5,6). Although commonly thought of as a woman's disease, it also occurs in men. In 2017, *in situ* breast carcinoma (no evidence of invasion) was diagnosed in about 63,410 women, while invasive breast carcinoma was diagnosed in about 252,710 women and 2,470 men in the United States of America. The number of breast cancer deaths was 40,610 women and 460 men. Despite the incidence of female breast cancer is rising and the incidence of male breast cancer is stable, the death rates declined due to improvements in early detection and treatment. Potential risk factors are: personal or family history of breast or ovarian cancer; inherited mutations in *BRCA1*, *BRCA2* or other breast cancer susceptibility genes; benign breast conditions, such as atypical hyperplasia; high breast tissue density; high natural levels of sex hormones; use of oral contraceptives; never having children; having the first child after age 30; long menstrual history; and postmenopausal hormone use. The most common symptom is a lump in the breast. Women with 40 or more years of age should do annual mammography, which is a low-dose x-ray procedure used to detect breast cancer at an early stage. Treatment usually involves either breast-conserving surgery (surgical removal of the tumor and surrounding tissue) or mastectomy (surgical removal of the breast), depending on tumor characteristics and patient preference. Axillary lymph nodes are generally removed and evaluated during surgery to determine whether the tumor has spread beyond the breast. Treatment may also involve (instead, before and/or after surgery) radiotherapy, chemotherapy, hormonal therapy or targeted therapy (7). Breast cancer recurrence can occur in two forms: distant metastasis and locoregional relapse. The late dissemination of cells that seed metastasis or local relapse suggests that they have most of the mutational processes active in the primary tumor. However, distant metastasis acquire diver mutations not seen in the primary tumor. Therefore, genome sequencing may help to decide the therapy (8). The 5-year relative survival rate in women for *in situ* and invasive breast carcinoma are 99% and 90%, respectively. However, men are more likely to be diagnosed at an advanced stage because of lack of awareness and screening for this disease. Therefore, the 5-year relative survival rate in men is 84% (7).

1.4 Molecular classification of breast cancer

Long before the advent of modern molecular profiling techniques, histopathologists recognized the heterogeneity of breast cancer through morphological observations, which was later confirmed through DNA microarrays. The identification of three markers (ER, PR and HER2) by gene expression profiling and immunohistochemistry, led to the classification of breast cancer into at least five subtypes: luminal A, luminal B, HER2, basal and normal (9).

Luminal breast cancers are the most common subtype, divided into luminal A and B, and expressing components of the luminal epithelial layer of normal breast ducts, such as *ESR1* (estrogen receptor), *LIV1* and *CCND1* (estrogen receptor activation), *GATA3*, *FOXA1*, *XBP1* and *cMYB* (10–12). Luminal tumors are often low grade, with fewer than 30% having mutations in p53 gene, i.e. substitutions that originate p53 protein with potential new functions (10,13). Luminal A tumors have, usually, higher expression of ER-related genes and lower expression of proliferative genes than luminal B tumors, carrying a significantly better prognosis. Therefore, luminal A tumors benefit from endocrine therapy alone, whereas luminal B tumors benefit from chemotherapy added to endocrine therapy (Table

1.1). Endocrine therapy blocks the body's ability to produce hormones or interferes with their activity (10,14).

The HER2-enriched subtype is characterized by low expression of ER and related genes, high expression of receptor tyrosine kinases, including FGFR4, EGFR, HER2 and genes within the HER2 amplicon (e.g. GRB7), and mutations in p53 gene (72%) (10–12). These tumors are high grade and poorly differentiated, with bad prognosis. Nevertheless, they are sensitive to HER2-molecular targeted agents and chemotherapy (Table 1.1) (10).

The basal-like subtype was so named because the expression pattern mimicked that of the normal basal/ myoepithelial breast cells (10). Of note, low-to-absent expression of HER2, ER, PR and p-cadherin/p63; high expression of HER1/EGFR, vimentin, c-Kit, cytokeratins 5/6, 14 and 17 (15). Tumors that are negative for HER2, ER and PR expression, are named triple negative. P53 mutations are the most frequent (80%), consisting of deletions/insertions that result in lack of p53 protein. Loss of p53 function through mutations in downstream effectors also occurs. In basal-like tumors, p53 regulates epithelial-mesenchymal transition and stem cell properties through upregulation of miR-200c. Loss of RB1 and BRCA1 functions are also common. Furthermore, many of the elements of the PI3K/AKT/mTOR and RAS/RAF/MEK/MAPK pathways are amplified (12,13). This subtype comprises high grade, ductal or metaplastic carcinomas that exhibit more marked nuclear pleomorphism, areas of central necrosis, high mitotic rates, a pushing border of invasion and a brisk lymphocytic infiltrate (15,16). The bad prognosis is due to inherent aggressiveness and poor therapy options in comparison to the other subtypes (10).

Unfortunately, a significant number of patients become resistant to the available treatments, so recent clinical trials are investigating molecular-targeted agents and combinatorial approaches (Table 1.1) (12).

Table 1.1: Therapeutic agents and corresponding mechanisms of action, specific to each breast cancer subtype. These therapeutic agents can be combined with conventional chemotherapy, especially in the case of basal-like tumors (12,14,15,17–20).

Luminal-like tumors		**HER2-enriched tumors**		**Basal-like tumors**	
Therapeutic agent	**Mechanism of action**	**Therapeutic agent**	**Mechanism of action**	**Therapeutic agent**	**Mechanism of action**
Goserelin (Zoladex®) and Leuprolide (Lupron Depot®)	Interfere with signals from the pituitary gland that stimulate the ovaries to produce estrogen.	Trastuzumab (Herceptin®)	Binds to the extracellular domain of HER2, triggering its internalization and degradation.	Cabozantinib (Cabometyx®) and Dasatinib (Sprycel®)	Inhibit multiple tyrosine kinases implicated in oncogenesis, tumor cell survival, angiogenesis, invasion and/or metastasis, including VEGFR, MET, RET and SRC.
Anastrozole (Arimidex®), Letrozole (Femara®) and Exemestane (Aromasin®)	Inhibit an enzyme called aromatase, which produces estrogen.	Lapatinib (Tyverb®)	Inhibits the intracellular ATP-binding site of the kinase domain of HER2.	OTX-015	Binds to bromodomain motifs of BET proteins, inhibiting their binding to acetylated histones, which occurs preferentially at super-enhancer regions that control oncogene expression.

Table 1.1 (continuation): Therapeutic agents and corresponding mechanisms of action, specific to each breast cancer subtype. These therapeutic agents can be combined with conventional chemotherapy, especially in the case of basal-like tumors (12,14,15,17–20).

Luminal-like tumors		HER2-enriched tumors		Basal-like tumors	
Therapeutic agent	**Mechanism of action**	**Therapeutic agent**	**Mechanism of action**	**Therapeutic agent**	**Mechanism of action**
Tamoxifen (Soltamox®), Toremifene (Fareston®) and Fulvestrant (Faslodex®)	Attach to ER, preventing estrogen from binding.	Pertuzumab (Perjeta®)	Binds to the extracellular dimerization domain of HER2, blocking its heterodimerization with other HER family.	Rucaparib (Rubraca®) and Olaparib (Lynparza®)	Inhibit PARP enzymes, which are involved in DNA repair, resulting in the formation of toxic PARP-DNA complexes, DNA damage and, ultimately, cell death.
Everolimus (Afinitor®)	Inhibits mTOR, since the PI3K/AKT/mTOR pathway promotes ER transcriptional activity.	Trastuzumab-DM1 (Kadcyla®)	Trastuzumab binds to HER2 and, upon internalization, DM1 is released and binds to tubulin, disrupting microtubule dynamics and inhibiting cell division.	Cetuximab (Erbitux®)	Attaches to EGFR, inducing its internalization and preventing its ligands from binding. EGFR is involved in cell survival, cycle, migration, invasion and angiogenesis.
Valproic acid (Depakene®)	Inhibits HDAC, which downregulates ER, epigenetically.	Tanespimycin and Ganetespib	Inhibit Hsp90, a ubiquitous molecular chaperone fundamental for correct folding and maturation of numerous cellular proteins, including HER2. In the absence of Hsp90 activity, HER2 is subject to proteolysis.	Scriptaid, Vorinostat (Zolinza®)	Inhibit HDAC, which downregulates tumor suppressor genes, as well as genes involved in cell cycle, proliferation, differentiation and apoptosis.

1.5 Cancer and DNA damage: an intimate relationship

Each of the approximately 10^{13} cells in the human body receives tens of thousands of DNA lesions per day (21). DNA damage can be generated spontaneously: dNTP misincorporation during DNA replication, interconversion between DNA bases caused by deamination, loss of DNA bases following depurination, modification of DNA bases by alkylation, oxidation of DNA bases and DNA breaks caused by reactive oxygen species derived from cellular metabolism. DNA damage can also be generated by environmental physical agents: ionizing radiation and ultraviolet light from the sun, clinical diagnosis employing X-rays or radiotherapy, which can originate pyrimidine dimers, photoproducts, oxidation of DNA bases, single-strand and double-strand breaks. Regarding environmental chemical agents: chemotherapeutic alkylating agents attach alkyl groups to DNA bases, crosslinking agents introduce covalent links between bases of the same or different DNA strands, and topoisomerase inhibitors induce the formation of single-strand and double-strand breaks by trapping topoisomerase-DNA complexes (22). However, cells have evolved mechanisms – collectively termed the DNA damage response – to detect DNA lesions, signal their presence and promote their repair (21). Normal cells harbor surveillance mechanisms, known as checkpoint pathways that control the entry and progression through the cell cycle, consisting of five phases: interphase, G_1, S, G_2 and mitosis (23). DNA-damage response factors arrest the cell cycle to provide ample time for the repair of DNA lesions before S-phase (G_1 arrest) and/or before mitosis (G_2 arrest) (24). The repair mechanisms employed depend on the DNA lesions: mismatch repair, base excision repair, nucleotide excision repair, single-

strand break repair, non-homologous end joining or homologous recombination (22). Faulty DNA damage response confers sensitivity to DNA damaging agents, which can be counteracted by the accumulation of mutations in genes implicated in cancer development and therapy resistance. However, extensive DNA damage ends up with cell death (25,26).

1.6 p53, guardian of the genome

P53 is a central player in tumorigenesis (27). Normally, p53 is bound to Mdm2, which inhibits its transcription-activating ability. In addition, Mdm2 has E3 ubiquitin ligase activity, catalyzing the ubiquitinylation of p53 and targeting it for proteasomal degradation (23). Upon DNA damage, p53 becomes phosphorylated on a serine residue in the N-terminus, which displaces Mdm2 and increases p53 levels (23,26). On the other hand, in the presence of aberrantly high (not persistent) oncogenic signaling (e.g. Myc, Ras), E2F transcription factor 1 induces ARF expression, which binds to and sequesters Mdm2 in the nucleolus (23,28). Finally, stabilized p53 binds to proteins involved in DNA repair (XPB, RPA and rad51) and activates transcription of p21, a cyclin-dependent kinase inhibitor, which binds to and inhibits various cyclin-cdk complexes that regulate mainly G_1-S but also G_2-M transition, arresting cells in G_1 phase before DNA replication and/or in G_2 phase before mitosis, for DNA repair (29). Of note, Mdm2 is transcriptionally activated by p53. Alternatively, cells become permanently arrested (senescence) or, when exposed to extensive DNA damage, are directed to apoptosis (23). Apoptosis occurs through the p53-induced release of cytochrome c, expression of pro-apoptotic BCL-2 family members (e.g. *puma*, *noxa*, *bid* and *bax*), components of death-receptor signaling (e.g. DR5 and Fas/CD95), the apoptotic effector machinery (e.g. caspase-6, Apaf-1 and PIDD) or others with less well-defined roles (e.g. PERP, PML and p53AIP) (28). The p53-mediated DNA damage response does not discriminate between damaged cells that are potential tumor cells and those that are not, causing the widespread pathologies following radiotherapy or chemotherapy (e.g. breathing problems, infertility, bowel changes, bladder inflammation, cognitive dysfunction and second cancer) (18,30). Inactivation of p53 leads to genomic instability since damaged DNA can replicate, accumulating mutations and rearrangements that are passed on to daughter cells at an increased rate, which contributes to tumorigenesis (23). Interestingly, prolonged metaphase arrest causes de-condensation of chromosomes and entry to "pseudo G1" phase at the tetraploid DNA content, followed by aberrant DNA replication, resulting in the formation of polyploid giant cells. The prevention of this phenomenon is mediated by p21, which acts in a similar way as in normal G1 phase to prevent replication of damaged DNA (29). Moreover, p53 can restrict chromosomal instability through its ability to cull cells at risk of aberrant mitosis, particularly following centrosome amplification and telomere dysfunction. Therefore, inactivation of p53 also deregulates the spindle assembly checkpoint, leading to chromosome mis-segregation and tetraploidization; allows cells to replicate and initiate chromosome breakage-fusion-bridge cycles, upon telomere dysfunction (31).

In a study performed by Silwal-Pandit and colleagues, approximately 28.3% of breast tumors presented p53 mutations. The majority of mutations were non-synonymous single base substitutions (73.4%) that result in full-length proteins with altered biological activity. Small deletions (18.7%) and insertions (5.2%) were predicted to encode truncated proteins. Complex mutations, comprising both deletions and insertions (2.0%), and tandem mutations (0.7%) were uncommon and of unclear biological significance. In addition, the p53 pathway may also be disrupted by allelic deletions (loss of heterozygosity) of p53 (32). Surprisingly, cancer cells drive selection for partial loss-of-function p53 mutations that retain pro-survival properties (30). Besides, certain p53 mutants bind p63 or p73, leading to changes in transcriptional profiles that alter receptor tyrosine kinase signaling to promote invasion and metastasis. Others cooperate with the SWI/SNF complex to upregulate the angiogenesis regulator VEGFR2 (31). Thus, the evolutionarily accreted multifunctionality of p53 has compromised its efficacy as a tumor suppressor (30).

1.7 NORAD, a lncRNA induced by DNA damage

To discover lncRNAs involved in the DNA damage response, Lee and colleagues analyzed a published dataset of murine lncRNAs induced by doxorubicin in a p53-dependent manner. A 4.9 kb transcript, annotated as *2900097C17Rik*, stood out because of its high conservation (approximately 65% nucleotides identity with its human ortholog, a 5.3 kb transcript, annotated as *LINC00657* and referred to as NORAD, which stands for non-coding RNA activated by DNA damage); high abundance (in humans approximately 300 to 1,400 copies per cell, like abundant housekeeping transcripts such as *ACTB*); ubiquitous expression across tissues and cell lines, at comparable levels, except for neuronal tissues and cell lines, where is more expressed; and predominant location in the cytoplasm (33,34).

This lncRNA is located in the chromosome 20q11.23, is intergenic, starts from a strong promoter overlapping a CpG island, the transcription start site is rich in H3K4me3-modified histones, the central 3.5 kb can be decomposed into 12 repeating units of approximately 300 nt each, terminates with a canonical poly(A) site and is unspliced. Some of these features indicate that NORAD is transcribed by RNA polymerase II. Within the repeats 1-10 are combinations of four sequence and structure conserved motifs: (i) one or two Pumilio recognition elements (PREs); (ii) a short-predicted stem-loop with four paired bases and a variable loop sequence; (iii) a U-rich stretch of 2-5 bases; and (iv) a stem-loop with eight or nine base pairs. Despite its p53-dependent induction, were not identified p53 binding sites in NORAD, suggesting indirect regulation (33,34).

1.8 Interaction with Pumilio proteins

PUMILIO 1 (PUM1) and PUMILIO 2 (PUM2) are highly conserved RNA-binding proteins, mainly located in the cytoplasm, that belong to the Pumilio-Fem3-binding factor (PUF) family, exhibiting 91% similarity in their RNA-binding domains and regulating almost the same set of targets. Pumilio proteins bind to an 8 nt specific sequence (UGUANAUA), named Pumilio recognition element (PRE), in the 3' untranslated region of target mRNAs, forming a multivalent cytoplasmic ribonucleoprotein (RNP) complex. Then, recruit 3' de-adenylation factors and antagonize translation induction by the poly(A) binding protein, or destabilize the 5' cap-binding complex, repressing gene expression. NORAD appears to be the preferred PUM2 target transcript and binds to it with great affinity because is composed of at least 17 Pumilio-binding motifs, mostly located in or near the conserved positions of the five repeated 400 nt Norad Domains (ND1 to ND5). The overall number of binding sites present in NORAD for Pumilio proteins (approximately 1,200) is comparable to their abundance in U2OS cells (approximately 200 and 550 copies per cell for PUM1 and PUM2, respectively). Upon DNA damage and in a p53-dependent manner, this lncRNA is activated and sequesters a significant fraction of the total cellular pool of Pumilio proteins, limiting the repression of target mRNAs involved in germline homeostasis, neuronal activity, mitosis, DNA repair and replication (Figure 1.1). Therefore, even small changes in NORAD levels can severely influence PUMILIO availability (33,34). Inactivation of NORAD results in PUMILIO hyperactivation and excessive repression of its targets, which perturb accurate chromosome segregation during mitosis, causing aneuploidy. Aneuploidy may contribute to gain of function of oncogenes and loss of function of tumor suppressor genes, leading to tumorigenesis. In this case, NORAD acts like a tumor suppressor gene. However, severe chromosome mis-segregations end up with cell death. In this case, NORAD acts like an oncogene (Figure 1.1). On the other hand, the canonical p53-dependent response is not affected (25,33). PUM1/2 overexpression not only results in changes in gene expression like those observed upon NORAD inactivation but also is sufficient to induce chromosomal instability (CIN) in $NORAD^{+/+}$ cells. CIN is the most common form of genomic instability, and comprises changes in chromosome number and structure. Conversely, PUM1/2 inactivation, significantly but not entirely, rescues chromosomal instability in $NORAD^{-/-}$ cells (33,35). Of note, Pumilio proteins were already detected in myeloid leukemia, non-small cell lung cancer, ovarian cancer, and their levels were positively associated with tumor stage. After interfering

with their expression, cell proliferation, clone formation, migration and invasion abilities were inhibited, while cell apoptosis was increased significantly. These results suggest that Pumilio proteins play an important role in tumorigenesis and progression (36). 90% of other PUM-bound transcripts have two or fewer PREs. Furthermore, the human genome contains at least 43 loci with NORAD-like sequences, which exhibit 84% - 98% identity to NORAD over approximately 500 bp. These sequences may serve as binding sites for other RBPs that may either facilitate the binding of PUM1/2 or affect its stability and activity. Therefore, NORAD also regulates the expression of genes that are not PUMILIO targets (33,34). In fact, an RNA-binding protein, SAM68 was found to bind to conserved secondary structures immediately downstream from the PREs in NORAD repeat units. It was also found to be required for efficient recruitment of PUM2 to NORAD, regulation of PUM activity by NORAD and proper chromosome segregation in mammalian cells (Figure 1.1). Interestingly, SAM68 may have an additional, NORAD-independent effect on PUM activity (37).

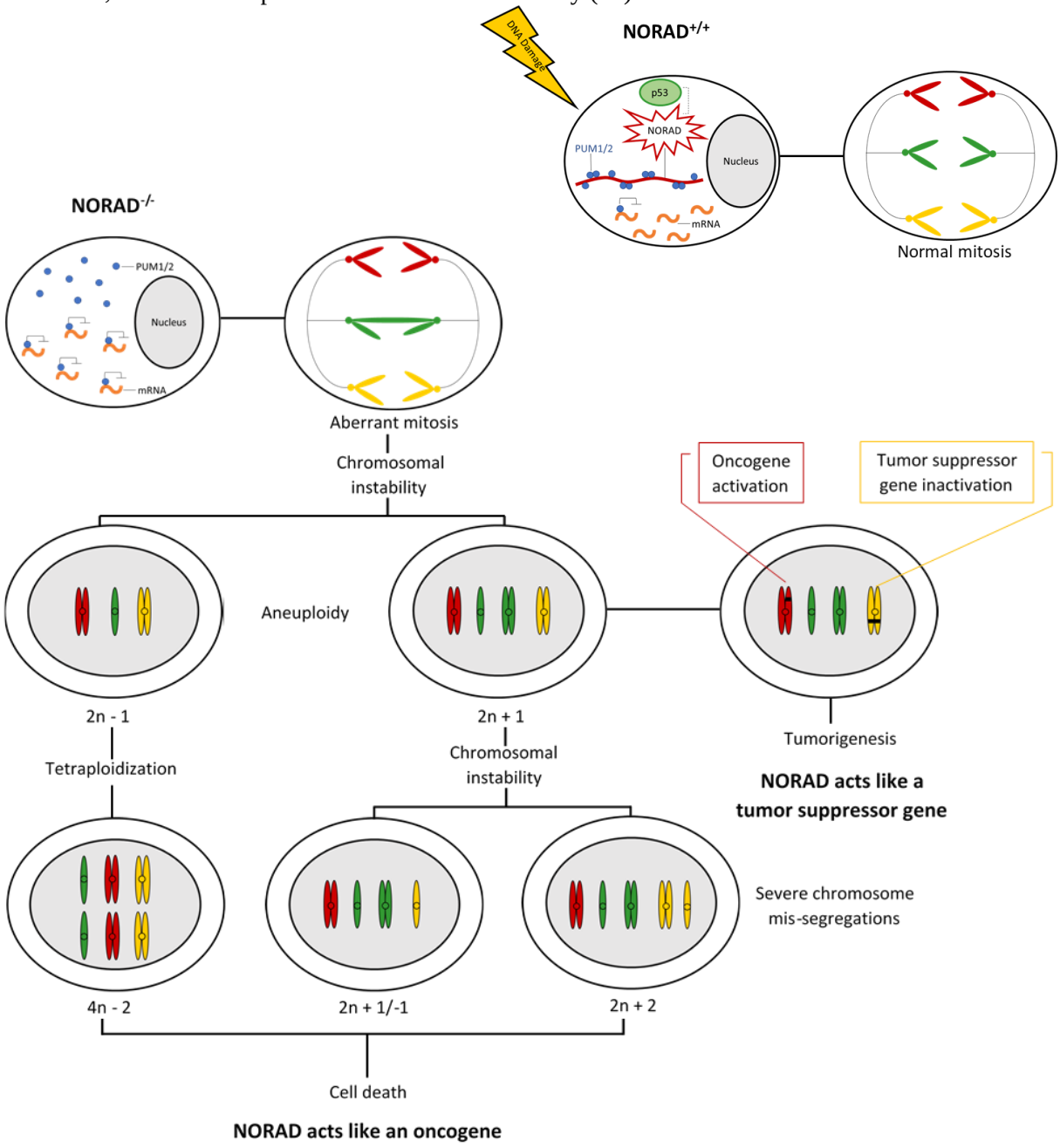

Figure 1.1: NORAD activation or inactivation and subsequent events. Upon DNA damage and in a p53-dependent manner, NORAD is activated and sequesters Pumilio proteins, limiting the repression of target mRNAs involved in mitosis, DNA repair

and replication. NORAD inactivation and subsequent repression of Pumilio proteins' target mRNAs, results in aneuploidy and tumorigenesis or severe chromosome mis-segregations and cell death (25,33,34,37).

1.9 NORAD expression profiles predicts clinical outcome in multiple human cancers

Liu and colleagues profiled cDNA arrays from OriGene consisting of 43 breast tumors and 5 normal breasts, and observed that in 9 of 43 samples (21%), *LINC00657* expression level was above a 2-fold of the mean expression level, which was associated with low overall survival (Kaplan-Meier test). They also found that expression of *LINC00657* was upregulated in breast cancer cell lines MCF-7 and MDA-MB-231, as compared to non-malignant human mammary epithelial cells (RT-qPCR). Therefore, *LINC00657* knockout by CRISPR/Cas9 in LM-4142, a derivative cell line from MDA-MB-231, caused significant reduction of cell viability (MTT assay) and number of colonies (clonogenic assay)(38).

In a study performed by Wu and colleagues, expression of NORAD was significantly upregulated in esophageal squamous cell carcinoma tissues (larger size and higher UICC stage) compared to adjacent normal tissues from 106 patients (RT-qPCR). Besides, patients with higher expression of NORAD had poorer overall survival and disease free survival (5-year follow-up, Kaplan-Meier test) (39).

Li and colleagues found that NORAD expression was significantly higher in 75 pancreatic cancer samples than in 55 normal pancreas tissues (GEO database), which was confirmed in 33 pancreatic cancer samples with complete clinicopathological information along with the corresponding normal pancreas tissues (RT-qPCR). Moreover, patients with higher NORAD expression had shorter overall survival and recurrence-free survival rates (Kaplan-Meier test). Therefore, NORAD knockdown using shRNAs markedly suppressed cell migration and invasion *in vitro* (wound healing, transwell migration and invasion assays), and *in vivo* since mice with NORAD expression presented more metastasis, including more distant metastasis (dual-luciferase reporter assay, hematoxylin and eosin staining) (40).

Furthermore, in a study performed by Bao and colleagues in endothelial cells, low concentration of oxLDL (oxidized low-density lipoprotein) induced oxidative stress and, consequently, expression of *LINC00657*. This lncRNA acted as a competing endogenous RNA inhibiting expression of miR-590-3p, which in turn suppressed HIF-1α. The upregulation of HIF-1α promoted expression of many growth factors and cytokines, including VEGF, MMP-2 and MMP-9, involved in cell survival (MTS assay), migration (wound healing and transwell assays) and tube formation (tube formation assay), ultimately leading to angiogenesis in atherosclerosis. miR590-3p was also found to participate in the carcinogenesis of different types of cancer such as prostate, liver and lung. Therefore, *LINC00657* might also induce angiogenesis in these tumors (41).

However, Hu and colleagues discovered that *LINC00657* was downregulated in hepatocellular carcinoma (HCC) tissues and cell lines (RT-qPCR), which was associated with high tumor size, vascular invasion, TNM stage and poor overall survival (tumor characterization, Kaplan-Meier test). Therefore, NORAD knockdown using shRNAs and siRNAs, promoted cell cycle (flow cytometry), proliferation (CCK-8 and colony-formation assays), migration and invasion (transwell chamber detection) *in vitro*, as well as tumor growth *in vivo* (tumor monitorization, H&E staining and immunohistochemistry) (42).

These results suggest that lncRNA NORAD expression or downregulation accounts for tumorigenesis and progression. Thus, it may represent a tumor marker for disease diagnosis, patient prognosis or therapy response, and it may represent a therapeutic target.

1.10 Long non-coding RNAs

Less than 2% of the genome encodes proteins, while at least 75% is transcribed into non-coding RNAs: short (sncRNAs) and long non-coding RNAs (lncRNAs) (43). Based on genomic organization and relationship to protein-coding genes, lncRNAs can be classified into: (1) sense or (2) antisense,

when overlapping one or more exons of another transcript on the same or opposite strand, respectively; (3) bidirectional, when its expression and of a neighboring coding transcript on the opposite strand are initiated in close genomic proximity; (4) intronic, when derived from an intron of a second transcript; or (5) intergenic, when it is an independent unit within the genomic interval between two genes (38,44). Generally, lncRNAs are defined by a length of >200 nucleotides and lack an open reading frame of significant length (less than 100 amino acids), are poorly conserved, less abundant and heterogeneous (33,45). However, the emerging evidence that some putative lncRNAs may encode short, translated open reading frames, and that coding RNAs can exert translation-independent functions, indicates that distinction between mRNA and lncRNA may be less absolute than once thought (46). Similarly to protein-coding genes, conservation is usually higher at the promoter regions of lncRNAs, which are enriched for A/T nucleotides and diminished in CpG patterns, and contain distinct transcription factor binding sequences and a unique pattern of chromatin marks, i.e., higher density of methylation at transcriptional start sites, regardless of expression levels (46). The lower levels of gene expression may not necessarily be the result of low RNA copy number in all cells, but may be the result from restricted expression in only a subpopulation of cells. Indeed, in a study performed by Djebali and colleagues, a considerable fraction (29%) of all expressed lncRNAs was detected in only one of the cell lines studied, whereas 10% were detected in all cell lines. Conversely, a considerable fraction (53%) of all expressed protein-coding genes were constitutive, whereas only 7% were cell-line specific (47). LncRNAs may be located in the nucleus, where regulate transcription, organize subnuclear structure and mediate chromosomal interactions, or in the cytoplasm, where modulate mRNA stability and translation, and influence cellular signaling cascades (33,39). The number of lncRNAs encoded by the genome has increased with animal evolution, suggesting that the presence of lncRNAs is linked to organismal complexity. Still, many human lncRNAs have syntenic orthologs in lower organisms (homologous genes present on the same chromosome, in different but related species). When performing comparative studies to analyze lncRNA conservation, should be taken into account that not just the sequence but also the structure, might determine function (43,48).

1.11 Mechanisms of action

LncRNAs function in the recruitment of protein factors for regulation of chromatin states. They may act as a scaffold onto which multiple protein complexes can assemble, recruit factors involved in gene activation or act as *cis*-acting molecular tethers. In fact, they are inherently attached to chromatin via DNA:RNA hybridization during transcription, are generally transcribed from a single locus in the genome, their length allows them to reach out and capture epigenetic complexes while tethered (either by Pol II or by bridging factors like YY1), and the unmasking of 3' degradation signals upon transcriptional termination would limit the RNA's half-life and prevent diffusion and action at ectopic sites. For example, *HOTAIR* interacts with the LSD1/CoREST/REST complex that demethylates histone H3K4 to prevent gene activation, synergizing the repressive effects of the PRC2 complex that also interacts with this lncRNA (49).

LncRNAs also directly affect the process of transcription, acting as decoys for transcription factors, transcriptional coregulators or inhibitors of Pol II activity. For example, lncRNAs transcribed from SINEs, an abundant class of retrotransposons, may block transcription of heat-shock genes by binding Pol II to prevent formation of preinitiation complexes (49).

In addition, they act in mRNA processing, stability and translation. For example, natural antisense transcripts may affect the alternative splicing of their overlapping transcripts by masking splice sites through base complementarity. For example, the α-thyroid hormone receptor gene *erbAα* produces two mRNA isoforms and has a downstream translated antisense transcript called *RevErb*, whose 3' untranslated region overlaps the last splice acceptor site of the long *erbAα* isoform, tilting the balance in favor of the short *erbAα* isoform (49).

Moreover, they are key regulators of nuclear compartments. For example, *MALAT1* interacts with the PRC1 subunit Cbx4/Pc2 and participates in the shuttling of genes between nuclear compartments for silencing and activation. In the presence of extracellular growth signals, unmethylated Cbx4 binds *MALAT1* and localizes its target genes, along with coactivating factors such as LSD1, to interchromatin granules that usually cluster around nuclear speckles, for transcription; in the absence of signal, Cbx4 becomes methylated, binds another lncRNA, *TUG1*, associates with corepressors such as Ezh2, and translocates to silencing compartments called Polycomb bodies (49).

Interestingly, the long and small ncRNA worlds intertwine. LncRNAs may interfere with miRNA-mediated mRNA destabilization by masking the binding sites for miRNAs or by sequestering miRNAs in their 3' untranslated regions that contain miRNA-binding sites. Moreover, lncRNAs can themselves be host genes for small RNAs. For example, in X chromosome inactivation, *Tsix* might repress *Xist* partly through an RNAi-related pathway, by base pairing to form an RNA duplex that yields Dicer-dependent small RNAs (siRNAs) (49).

However, in some cases it may be the act of transcription, and not the transcript itself, that is important. For example, in the control region of the β-globin locus, polyadenylated transcripts of varying lengths are generated from the HS2 enhancer site. No biological function is ascribed to these transcripts, but because HS2 is unable to activate globin expression when a transcriptional terminator is placed between it and the globin promoter, the phenomenon is interpreted to be transcription rather than transcript dependent. Indeed, intergenic transcription occurs throughout the globin locus and plays a role in establishing open chromatin domains marked by permissive histone modifications such as H3K4me2/3 and H3 acetylation (49).

1.12 LncRNA-based diagnostics and therapies in cancer

LncRNAs have key roles in gene regulation and, consequently, affect various aspects of cellular homeostasis, including proliferation, survival, migration or genomic stability. Cancer is primarily caused by genetic alterations that result in the deregulation of the gene networks that are responsible for the maintenance of cellular homeostasis. In addition, tumor suppressor genes and oncogenes may regulate the transcription of lncRNAs. For their application as biomarkers, lncRNAs should present tissue- and cell type-specific expression and, should be stable and easily detectable in body fluids to permit noninvasive diagnosis (43). For example, the lncRNA *PCA3* is a specific and sensitive marker of prostate cancer in patient urine samples, which was the first Food and Drug Administration-approved test based on a lncRNA (46). Similarly, the lncRNA *HULC* is highly expressed in patients with hepatocellular carcinoma and can be detected in the blood by conventional PCR methods. Since lncRNAs regulate specific facets of protein activity, they also represent potential therapeutic targets. Of note, drugs that target lncRNAs can be more refined and less toxic than conventional protein-targeting drugs (43). Some therapeutic strategies utilize oligonucleotides for the knockdown of lncRNAs. siRNAs consist of an antisense (or guide) strand and a sense (or passenger) strand, forming a duplex 19 to 25 bp in length with 3' dinucleotide overhangs, and are mainly located in the cytoplasm. When bound by Argonaut 2 in the RNA-induced silencing complex, the passenger strand is discarded, leaving the guide strand free to bind an RNA target that is subsequently degraded (50,51). Alternatively, LNA™ GapmeRs are antisense oligonucleotides enriched with locked nucleic acids in the flanking regions and DNA in a central region, and are mainly located in the nucleus. The locked nucleic acids-containing flanking regions confer nuclease resistance and increase target binding affinity; the central DNA activates RNase H-cleavage of the target RNA upon binding (51,52). Still, LNA™ GapmeRs share some limitations with siRNAs: inefficient delivery, incomplete knockdown, off-target effects and temporary inhibition. On the other hand, genome-editing methods, such as transcription activator-like effector nucleases (TALENs) and clustered regulatory interspaced short palindromic repeats (CRISPR) – associated endonuclease 9 (Cas9), could be effective for stable knockdown of lncRNAs. Moreover, features of

lncRNAs can be exploited for other therapeutic strategies that do not necessarily involve targeting them. The plasmid BC-819 (DTA-H19) was developed to carry the gene for the A subunit of diphtheria toxin under the regulation of the promoter of the H19 lncRNA with tumor-specific expression. Intratumoral injection induces the expression of high levels of diphtheria toxin, resulting in a reduction of tumor size in human trials in a broad range of carcinomas and reduction of the risk of affecting normal tissues (43).

1.13 Chemotherapy

Chemotherapy is the use of drugs to treat cancer. Selectivity towards cancer cells occurs because of their higher proliferation relative to normal cells, with the exception of cells from the bone marrow, gastrointestinal mucosa and hair follicles. However, since drugs cannot distinguish between normal and cancer cells, common side-effects include myelosuppression, nausea, vomiting and hair loss. Moreover, cancer cells are often defective in their ability to repair DNA damage (53). Once chemotherapeutic agents are rapidly eliminated from the systemic circulation, high doses are required for antitumor efficacy. Only a small number of cancer types can be cured with chemotherapeutic agents (e.g. childhood blastomas) (54). Tumors can be intrinsically resistant to chemotherapy before treatment or acquire resistance during treatment (35). Chemotherapeutic agents are divided into: alkylating agents, platinum compounds, antimetabolites, anthracyclines, topoisomerase inhibitors, tubulin-binding drugs and tyrosine kinase inhibitors (55).

Adriamycin (generic name doxorubicin) is an anthracycline isolated from the bacterium *Streptomyces peucetius var. caesius*, and is the hydroxylated congener of daunorubicin (56). This drug is used for treatment of solid tumors arising in the breast, bile ducts, endometrial tissue, esophagus and liver, osteosarcomas, soft-tissue sarcomas and non-Hodgkin's lymphoma (57). It is known that doxorubicin intercalates between base pairs in DNA, preventing DNA replication and protein synthesis; inhibits topoisomerase II, resulting in an increased and stabilized cleavable enzyme-DNA linked complex during DNA replication and in the non-repair of double-strand breaks (56). However, a new mechanism of action has been recently revealed, which depends on a transmembrane precursor, cAMP response element-binding protein 3-like 1 (CREB3L1), with a transcription factor domain located in the N terminus that projects into the cytosol, while the C terminus projects into the lumen of the endoplasmic reticulum. Doxorubicin induces the synthesis of ceramide that triggers the transportation of CREB3L1 from the ER to the Golgi complex, where occurs the regulated intramembrane proteolysis of CREB3L1, which releases the N terminus, allowing translocation to the nucleus and transcription of genes that suppress cell proliferation (58,59). These genes encode cyclin inhibitors p21 and p18, c-myc antagonists Mxi-1, GADD45γ, SPARC and RGC32 (60). The major side effect is cardiotoxicity associated with oxygen free radical formation from reduced doxorubicin intermediates (61).

1.14 Combinatorial approaches

The discoveries on the molecular mechanisms of cancer development have prompted the search for agents that interfere with pathways controlling cancer cell survival, proliferation and invasion, reducing the toxicity to normal cells (62). However, considering the heterogeneity of tumors, acting in only one pathway is not an effective treatment (63). Therefore, the combination of conventional chemotherapeutic agents with novel molecular-targeted agents might be a promising therapeutic approach. First, since the targets and mechanisms of action of these agents are different, there is no cross-resistance. Second, since in combinatorial approaches, the concentrations are low, chemotherapeutic agents side effects and molecular-targeted agents off-target effects are reduced. Third, alterations in expression and/or activity of genes that regulate mitogenic signals caused by molecular-targeted agents, not only may perturb cell growth but also may reduce resistance and sensitize cancer cells to chemotherapeutic agents (54,62). For example, the chemotherapeutic agent 5-fluorouracil (5FU) creates fluorinated nucleotides that are incorporated into DNA in place of thymidine, inhibiting DNA

replication and causing cell death. The lncRNA HOTAIR contributes to colorectal cancer and 5FU resistance through the recruitment of EZH2, epigenetic silence of miR-218, upregulation of VOPP1 expression and subsequent activation of the NF-kB/TS pathway. Thus, suppression of HOTAIR results in sensitivity to 5FU (64).

2. Objectives

The recently discovered human lncRNA NORAD is induced after DNA damage in a p53-dependent manner and plays a critical role in the maintenance of genomic stability. NORAD inactivation results in chromosomal instability and aneuploidy, which contributes to tumorigenesis or severe chromosome mis-segregations and cell death. Moreover, it has been detected in several types of cancer. In breast cancer, pancreatic cancer and esophageal squamous cell carcinoma, the lncRNA expression is upregulated and its knockdown inhibits cell viability, proliferation, migration and invasion. However, in hepatocellular carcinoma the lncRNA expression is downregulated and its knockdown promotes cell cycle, proliferation, migration and invasion. Having this in mind (NORAD action as an oncogene or tumor suppressor gene and contradictory results in different types of cancer), the main aim of the present study was to unravel the role of this lncRNA in breast cancer, which is the most frequently diagnosed and the second-leading cause of cancer death in women, in order to ascertain if it represents a potential therapeutic target.

Hence, mRNA basal levels of NORAD were determined in a set of human epithelial breast cancer cell lines (MCF-7, MDA-MB-231, 468 and 436) in comparison to a non-malignant human mammary epithelial cell line (MCF-10A). Correlation between the lncRNA expression levels and patients prognosis was also established. Then, its knockdown was performed and tumor-relevant phenotypes (cell viability, cycle, migration and apoptosis) were analyzed.

Another goal of this project was to explore the p53 pathway since it is a tumor suppressor gene, considered as the guardian of the genome, which also plays an important role in response to DNA damage. Understanding how it works may help to explain some of the effects observed upon NORAD knockdown. Therefore, mRNA and proteins levels were determined in different conditions.

Finally, due to the increasing number of resistance cases to chemotherapy, it was also important to evaluate, for the first time, the outcome of combining NORAD knockdown with chemotherapeutic agents i.e. if NORAD knockdown increases the sensitivity of human epithelial breast cancer cell lines to chemotherapeutic agents, in this case doxorubicin which is used in breast cancer management in the clinical setting.

3. Materials and methods

3.1 Cell culture

The non-malignant human mammary epithelial cell line MCF-10A was generously offered by Doctor Sérgio de Almeida (Instituto de Medicina Molecular/João Lobo Antunes, Lisbon). The human epithelial breast cancer cell lines MDA-MB-231, 436, 468 and MCF-7 were generously offered by Doctor Sérgio Dias (Instituto de Medicina Molecular/João Lobo Antunes, Lisbon) and are characterized in Table 3.1. MCF-10A cells were cultured in DMEM/F-12 (Dulbecco's Modified Eagle Medium/Nutrient Mixture F-12, Gibco by Life Technologies), supplemented with 5% v/v horse serum (Gibco by Life Technologies), epidermal growth factor (20 ng/mL) (Millipore), hydrocortisone (0.5 µg/mL), cholera toxin (100 ng/mL), insulin (10 µg/mL) and 1% v/v penicillin-streptomycin (Gibco by Life Technologies). MDA-MB-231, 436, 468 and MCF-7 cells were cultured in DMEM (Gibco by Life Technologies), supplemented with 10% v/v heat inactivated fetal bovine serum (FBS), 1% v/v L-glutamine and 1% v/v penicillin-streptomycin (Gibco by Life Technologies). All cells were maintained at 37°C in a humidified atmosphere (90%) containing 5% CO_2, at the exponential growth phase under

adherent conditions. All cells were visualized and photographed in a Primo Vert inverted microscope (Carl Zeiss) incorporated with an AxioCam ER c5s.

Table 3.1: Characterization of the human epithelial breast cancer cell lines used in this study. MCF-7 cells belong to the luminal subtype and present a wild-type p53 gene sequence, while MDA-MB-231, 468 and 436 cells belong to the tripe negative subtype, which is the most aggressive, and present p53 mutations (5,9,65,66).

Cell line	Tumor type	Origin of cells	Receptor status Morphology	P53 gene
MDA-MB-231	Adenocarcinoma	Pleural effusion	Triple negative Mesenchymal-like	Missense mutation
MDA-MB-468			Triple negative Basal-like	
MDA-MB-436	Invasive ductal carcinoma		Triple negative Mesenchymal-like	Truncating mutation
MCF-7			ER: + PR: +/- HER2: - Luminal-like	Wild-type

3.2 RNA isolation, cDNA synthesis and RT-qPCR

Total RNA was isolated using NZYol, following manufacturer's instructions (NZYTech). RNA quantity and quality was verified by measuring the absorbance at 230nm, 260nm and 280nm using NanoDrop 2,000 Spectrophotometer (Thermo Fisher Scientific). Ideally, the $A_{260/280}$ and $A_{260/230}$ ratios should be between 1.8 and 2.0. cDNA synthesis was performed with 200ng - 1µg of RNA and random hexamers using the Roche Transcriptor High Fidelity cDNA Synthesis Kit. The program on thermocycler consists of 10 minutes at 65°C (annealing of primers), 10 minutes at 29°C (extension of primers), 60 minutes at 48°C (cDNA synthesis) and 5 minutes at 85°C (degradation of other RNA and DNA molecules). Finally, real-time quantitative reverse transcriptase polymerase chain reaction (RT-qPCR) was performed in the ViiA 7 Real-Time PCR System (Thermo Fisher Scientific) using SYBR Green PCR master mix (Thermo Fisher Scientific). The program consists of 40 cycles: 2 minutes at 50°C (stage 1 – initial denaturation), 10 minutes at 95°C (stage 2 – dissociation of dsDNA into ssDNA), 15 seconds at 95°C and 1 minute at 60°C (stage 3 – annealing and extension of primers), 15 seconds at 95°C, 1 minute at 60°C and 15 seconds at 95°C (stage 4 – dissociation of dsDNA with incorporated dye molecules into ssDNA, melting curve). For results analysis, a comparative quantification between the threshold cycle (C_t) values of the genes of interest (NORAD and p53) in both the test sample and calibrator sample (e.g. untreated), and the C_t values of the housekeeping genes (β-actin and 18S) in the same two samples, was performed using the $2^{-\Delta\Delta Ct}$ method. Gene-specific primer pairs (Sigma-Aldrich) (10 µM) and sequences are presented in Table 3.2. Primer pairs efficiency was tested.

Table 3.2: Gene-specific primer pairs and sequences used in RT-qPCR. The genes of interest are NORAD and p53, while the housekeeping genes are β-actin and 18S.

NORAD 1	Forward: 5' – TGTTTGTGCAGTGGTTCAGG – 3' Reverse: 5' – TCTTGCCTCGCTGTAAACAG – 3'
NORAD 2	Forward: 5' – AAAGTGTACAACGGCCTGTC – 3' Reverse: 5' – ATGGGGTTTCACCATGTTGG – 3'
NORAD 3	Forward: 5' – AGCGAAGTCCCGAACGACGA – 3' Reverse: 5' – TGGGCATTTCCAACGGGCCAA – 3'
p53	Forward: 5' – CCCCTCCTGGCCCCTGTCATCTTC – 3' Reverse: 5' – GCAGCGCCTCACAACCTCCGTCAT – 3'
β-actin	Forward: 5' – TGACGTGGACATCCGCAAAG – 3' Reverse: 5' – CTGGAAGGTGGACAGCGAG – 3'
18S	Forward: 5´ – GGATGTAAAGGATGGAAAATACA – 3' Reverse: 5' – TCCAGGTCTTCACGGAGCTTGTT – 3'

3.3 Single-molecule RNA fluorescence *in situ* hybridization (smRNA FISH)

Stellaris® FISH probes recognizing NORAD and labeled with Quasar® 570 dye were purchased from Biosearch Technologies, Inc.. The probe set sequences utilized in the experiments had been previously described and each set comprises 48 different oligonucleotides (20 nucleotides in length each) (33).

Cells were seeded on gelatin- or polylysine-coated glass coverslips in flat-bottom 24-well plates. After treatment, cells were washed in 1x phosphate-buffered saline (PBS) and fixed with 3.7% paraformaldehyde (PFA) for 10 minutes at RT. Fixed cells were then washed in 1x PBS, permeabilized in 70% ethanol for 1 hour at RT and in 0.1% tween 20 or 0.1% triton X-100 for 15 minutes at RT, and washed with wash buffer containing 80% of 20x saline sodium citrate (SSC), 10% deionized formamide (FA) and 10% nuclease-free water. Within a humidified chamber, coverslips were transferred to hybridization buffer (20% of 50% dextran sulfate, 10% of 20x SSC, 10% deionized formamide and 60% nuclease-free water) containing 1% probe, left overnight at 37°C, washed with wash buffer and 2x SSC. Finally, the coverslips were mounted in vectashield mounting medium with DAPI (4', 6-diamidino-2-phenylindole) (2µg/mL). Images were acquired with a laser-scanning confocal inverted microscope (LSM710; Carl Zeiss), 63x oil-immersion objective (NA 1.4), in z-stack with maximum intensity projection, using ZEN software.

3.4 NORAD knockdown

Gene knockdown was achieved using 2 LNA™ GapmeRs (Exiqon) at a final concentration of 25nM, and a SMARTpool of 4 siRNAs (Dharmacon) at a final concentration of 25 nM, that target different regions of NORAD. LNA™ GapmeRs were designed using the antisense LNA™ GapmeR design tool and present the following sequences: 5' – CTAGACGTAAATTAGG – 3' (human NORAD LNA™ GapmeR 1) and 5' – ACTTTACTAAAAACGC – 3' (human NORAD LNA™ GapmeR 3). As control was used a LNA™ GapmeR at a final concentration of 50 nM and a siRNA at a final concentration of 25 nM, directed to non-specific sequences. LNA™ GapmeRs and siRNAs were resuspended in DNase RNase free H_2O at a stock concentration of 50 µM and a working concentration of 10 µM. Initially, cells were seeded to be 60 – 80% confluent for transfection. In a 1.5 mL eppendorf a, lipofectamine® RNAiMAX transfection reagent (Invitrogen) was diluted in opti-MEM® (serum-free medium); in eppendorf b, LNA™ GapmeRs and siRNAs were diluted in opti-MEM®. Next, the content of eppendorf a was transferred to eppendorf b, vortexed and incubated at RT for 15 minutes. Finally, cells were transfected with the lipid complexes (dropwise). A second transfection was performed 24 or 48h after the first transfection. Cells were analyzed 24, 48 or 72h after transfections (transient effect). Of note, the volume of transfection solution should not correspond to more than 10% of the final volume of culture medium in the wells of the plate.

3.5 Cell viability

Culture medium containing 10% (v/v) alamarBlue® cell viability reagent (Thermo Fisher Scientific) was added to the cells for the alamarBlue® reduction assay. AlamarBlue® consists in an oxidation-reduction (REDOX) indicator used for quantitative analysis of cell viability, which changes from an oxidized (non-fluorescent, blue) form to a reduced (fluorescent, red) form, in response to chemical reduction of growth medium resulting from cell growth. Plates were incubated for approximately 2 hours, protected from light, until a color change was detected for the untreated cells (condition expected to present the highest cell viability), and the fluorescence intensity was measured in a plate-reading fluorometer (Microplate Reader Infinite M200, Tecan) with excitation wavelength at 560nm and emission wavelength at 590nm. Cell viability was calculated as a percentage of control cells using the Equation 3.1:

$$Cell\ viability\ (\%) = \frac{\text{Fluorescence Intensity 590 nm Treated Cells}}{\text{Fluorescence Intensity 590 nm Control Cells}} \text{ x } 100 \quad \text{(Equation 3.1)}$$

The control cells were treated with medium alone.

3.6 Cell migration

Cells were seeded in a 12-well plate at a density of 160,000 cells/well and transfected for NORAD knockdown, as previously described (two transfections with a 48h interval). When cells reached confluence, was added fresh medium with mitomycin C at 0.5 μM to inhibit cell proliferation. After 1h, cells were washed with PBS and was added fresh medium. After 1h, a scratch was performed in each well with P1000 filter tips, cells were washed with PBS and was added fresh medium. After 1h, were taken pictures of each well at different time points (t = 0, 6, 12, 24, 48h), using a Primo Vert inverted microscope (Carl Zeiss) incorporated with an AxioCam ER c5s (4x objective). The width of the scratch was measured using ImageJ software and the migration rate was calculated relative to the time point t = 0h.

3.7 Assessment of doxorubicin IC_{50}

Doxorubicin (Sigma-Aldrich, D2975000) was resuspended in dH_2O at a stock concentration of 5 mM and diluted to a working concentration of 50 μM. Cells were seeded in 48-well plates at a density of 40,000 cells/well. 48h after plating, cells were incubated with doxorubicin in a range of concentrations (0.0625, 0.125, 0.25, 0.5, 1, 2, 4, and 8 μM). 24h after incubation with doxorubicin, the medium was replaced with fresh medium and 48h after incubation with doxorubicin, was performed the alamarBlue® reduction assay. The required drug concentration to promote reduction of 50% in cell viability (IC_{50}) was determined from non-linear curve fit assuming sigmoidal dose-response in GraphPad PRISM software.

3.8 Combination studies with NORAD knockdown and doxorubicin

Cells were seeded in 48-well plates at a density of 25,000 cells/well and transfected for NORAD knockdown, as previously described (two transfections with a 24h interval). In order to evaluate if NORAD knockdown sensitizes cancer cells to chemotherapy, 48h after plating, cells were incubated with doxorubicin in a range of concentrations (0.1, 0.2, 0.4, 0.8, 1.6 and 3.2 μM). 24h after incubation with doxorubicin, the medium was replaced with fresh medium and 48h after incubation with doxorubicin, were performed analysis of cell viability, cell apoptosis and cell cycle.

3.9 Protein isolation and western blot

Total protein was isolated using NZYol, following TRIzol manufacturer's instructions for protein isolation (Invitrogen), and was resuspended in 2x sample buffer (80mM Tris HCl, 16% glycerol, 4.5% SDS, 150mM dithiothreitol and 0.01% bromophenol blue). Protein quantity was assayed by running samples mixed with a protein dye, on a SDS-PAGE (sodium dodecyl sulphate-polyacrylamide gel electrophoresis) gel, followed by Coomassie blue staining (0.25g Comassie, 50mL methanol, 10mL acetic acid to 100mL) for 30 minutes and destaining (10mL acetic acid, 10mL methanol to 100mL) till clear blue bands on clear background are visible. For western blot, samples were loaded on a 10% SDS-PAGE gel composed by stacking (1.2mL 30% Acrylamide/bis, 2mL S gel buffer (0.5M Tris pH 6.8 and 0.4% SDS), 4.7mL H_2O, 40μL Temed and 40μL 10% APS, for 2 gels) and running gel (3.3mL 30% Acrylamide/bis, 2.5mL R gel buffer (1.5M Tris pH 8.8 and 0.4% SDS), 4.2mL H_2O, 40μL Temed and 20μL 10% APS, for 2 gels). The SDS-PAGE gel was placed on an electrophorator (BioRad) filled with 1x running buffer (5x running buffer: 30.25g Tris, 144g glycine, 5g SDS to 1L) and connected to a power source (BioRad) initially at 90V and then at 120V for 1h. Next, was performed electrotransfer from the SDS-PAGE gel to a nitrocellulose membrane, making a sandwich formed by sponge, two filter

papers, nitrocellulose membrane, SDS-PAGE gel, two filter papers and sponge, all wet on transfer buffer (2.9g 24mM Tris, 14.5g 193mM glycine, 200mL 20% methanol to 1L). The sandwich was placed on the transfer apparatus filled with transfer buffer and connected to a power supply at 300mA, 4ºC, for 90 minutes. The membrane was washed with 1x PBS, stained with Ponceau red solution for 30 minutes and destained, to confirm that the transfer was well succeeded. The membrane was washed with 1x PBS, blocked with 10% milk for 30 minutes, washed with 1x PBS and incubated with primary antibodies for 1h on a shaker. The membrane was washed with 0.05% PBS-tween, incubated with secondary antibodies for 1h and washed once again with 0.05% PBS-tween, on a shaker. SuperSignal® West Femto Maximum Sensitivity Substrate (ThermoFisher Scientific) or Amersham™ ECL™ Western Blotting Detection Reagents (GE Healthcare) were used to detect the signal emitted by the antibodies on Curix 60 (Agfa) with medical x-ray film blue (Agfa) in the dark room, or on ChemiDoc™ XRS+ (BioRad). Protein-specific antibodies are presented in Table 3.3.

Table 3.3: Protein-specific antibodies used in western blot. The proteins of interest are p53 and γH2AX, while the housekeeping protein is β-actin.

Protein	Primary antibody	Secondary antibody
p53	Abcam ab1101 1:500	Goat Anti-Mouse IgG (H+L)-HRP Conjugate (Jackson ImmunoResearch) 1:4000
γH2AX	Abcam ab2893 1:500	Goat Anti-Rabbit IgG (H+L)-HRP Conjugate (BioRad) 1:3000
β-actin	Sigma-Aldrich A5441 1:3000	Goat Anti-Mouse IgG (H+L)-HRP Conjugate (Jackson ImmunoResearch) 1:4000

3.10 Cell apoptosis

Cell apoptosis analysis was performed using the Annexin V-CF Blue/7-AAD (aminoactinomycin D) Apoptosis Detection Kit (Abcam ab214663). Cells were trypsinized, centrifuged at 1,200 rpm during 5 minutes, washed with 1x PBS, centrifuged once again and resuspended in 1x Binding Buffer Solution at a final concentration of 1 x 10^6 cells/mL. To each 100µL of cell suspension, were added 2.5µL of Annexin V-CF Blue Conjugate and 5µL of 7-AAD Staining Solution. After incubation at RT for 15 minutes in the dark, were added 400µL of 1x Binding Buffer Solution, cells were transferred to FACS tubes and analyzed in the BD LSRFortessa™ X-20 cytometer. Annexin V is a protein with high affinity for phosphatidylserine (PS) that occurs on the external surface of the cell membrane in the early phases of apoptotic cell death, during which the cell membrane remains intact. 7-AAD is a membrane impermeant dye, generally excluded from viable cells, that binds to dsDNA by intercalating between base pairs in GC-rich regions. Simultaneous staining of cells with Annexin V-CF Blue (blue fluorescence, Ex/Em max = 408/450 nm) and 7-AAD (red fluorescence, Ex/Em max = 543/647 nm) allows the discrimination of intact cells (Annexin V-CF Blue negative, 7-AAD Staining Solution negative), early apoptotic (Annexin V-CF Blue positive, 7-AAD Staining Solution negative) and late apoptotic or necrotic cells (Annexin V-CF Blue positive, 7-AAD Staining Solution positive). Results were analyzed using the FlowJo software.

3.11 Cell cycle

Cells were trypsinized, centrifuged at 1,200rpm for 5 minutes, washed with 1x PBS and centrifuged. For the fixation and permeabilization steps, 70% ethanol was added dropwise while vortexing, with posterior incubation for 30 minutes at RT. Cells were centrifuged at 1,200rpm for 5 minutes, washed with 1x PBS and centrifuged once again. Finally, cells were resuspended in 300µL of staining buffer (PBS + 5% FBS) with 5µL of propidium iodide (1 mg/mL) (equivalent to 7-AAD),

transferred to FACS tubes and analyzed in the BD LSRFortessa™ X-20 cytometer. Results were analyzed using the ModFit software.

3.12 Statistical analysis

All results are represented as an average ± standard deviation (SD) of at least two independent experiments with biological and technical duplicates or triplicates. Graph construction and statistical analysis were performed in GraphPad Prism software, using one-way ANOVA. In all results: no-symbol $p>0.05$, * $p<0.05$, ** $p<0.01$ and ***$p<0.001$.

4. Results and discussion

LncRNAs have emerged as regulators of diverse biological processes. The recently discovered human lncRNA NORAD is induced after DNA damage in a p53-dependent manner and plays a critical role in the maintenance of genomic stability (33). It has been detected in several types of cancer, including breast cancer, which is the most frequently diagnosed and the second with the highest mortality in women (5,6,38). Therefore, NORAD caught our attention for its potential use as a therapeutic target.

4.1 NORAD and p53 expression profiles in human epithelial breast cancer cell lines

Initially, mRNA basal levels of NORAD were determined in a set of human epithelial breast cancer cell lines (MCF-7, MDA-MB-436, 468 and 231) and in a non-malignant human mammary epithelial cell line (MCF-10A) for comparison, through real-time quantitative reverse transcriptase polymerase chain reaction (RT-qPCR), and was observed that MDA-MB-436, 468 and 231 cell lines, which belong to the most aggressive triple negative subtype, tend to express higher levels of NORAD, while MCF-7 cell line, which belongs to the luminal subtype, tends to express NORAD at comparable levels with MCF-10A cell line. Therefore, this lncRNA may represent a tumor marker for disease diagnosis (Figure 4.1). Liu and colleagues have previously demonstrated upregulated expression of NORAD for MCF-7 and MDA-MB-231 cell lines, as well as for breast tumor tissues (38). Similar results were obtained for esophageal squamous cell carcinoma and pancreatic cancer, and opposite results were obtained for hepatocellular carcinoma (39,40,42). The lack of significant results (except for the MDA-MB-468 cell line) may be related to the variability inherent to each experiment or cell confluence before lysis, which may influence mRNA synthesis (Figure 4.1).

Iyer and colleagues analyzed poly A^+ RNA-seq data from more than 7,000 samples (including normal and tumor cell lines and tissues) and found that the expression of 8,000 of a total of 58,000 lncRNAs was associated with cancer. However, it remains to be determined if they play a critical role in oncogenesis (67). The first lncRNAs that were associated with cancer because of their aberrant expression were prostate cancer associated 3 (PCA3) and prostate-specific transcript 1 (PCGEM1). PCA3 is currently used as a prostate cancer biomarker and PCGEM1 is involved in androgen receptor transcriptional activation and c-MYC activation, both important for the development of prostate cancer (43).

mRNA basal levels of p53 were also determined through RT-qPCR because it is a tumor suppressor gene, considered as the guardian of the genome, that plays an important role in response to DNA damage, such as NORAD activation (33,68). It was observed that MDA-MB-436, 468 and 231 cell lines express low levels of p53, while MCF-7 cell line expresses high levels of p53 (Figure 4.1). These results might be explained by the identification of a wild-type p53 gene sequence for MCF-7 cell line, missense mutation for MDA-MB-468 and 231 cell lines, and truncating mutation for MDA-MB-436 cell line (66). Despite the presence of a wild-type p53 gene sequence, MCF-10A cell line expresses low transcript levels because it is not activated in the absence of stress conditions or oncogenic signaling (Figure 4.1) (23,26,28).

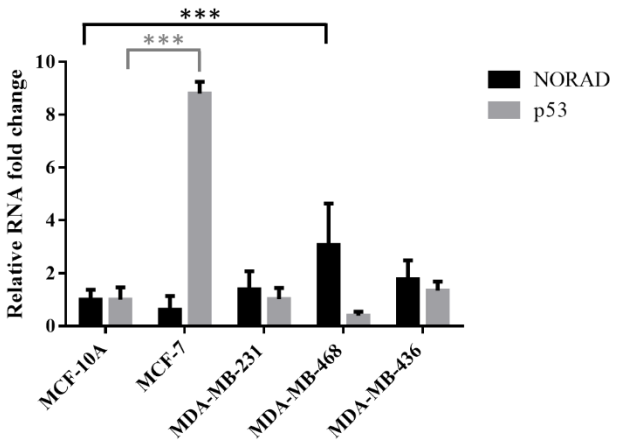

Figure 4.1: NORAD and p53 mRNA basal levels in human epithelial breast cancer cells. RT-qPCR was performed, using pair of primers NORAD1 for the gene of interest and β-actin as housekeeping gene. For statistical analysis was used one-way ANOVA, with the non-malignant human mammary epithelial cell line (MCF-10A) for comparison. No-symbol $p>0.05$, ***$p<0.001$.

4.2 NORAD is predominantly cytoplasmic

In order to visualize the subcellular localization of NORAD, was performed single-molecule RNA fluorescence *in situ* hybridization (smRNA FISH) with probe set sequences previously described by Lee and colleagues. NORAD localizes almost exclusively in the cytoplasm, as previously described in U2OS (osteosarcoma), HCT116 (colon carcinoma) and other cell lines through smRNA FISH, subcellular fractionation and EMBL-EBI Expression Atlas, with approximately 94% of NORAD copies located in the cytoplasm and 6% in the nucleus (Figure 4.2). Cytoplasmic lncRNAs modulate the activity or abundance of interacting proteins or mRNAs. In this case, NORAD interacts with Pumilio proteins, limiting the repression of their target mRNAs involved in germline homeostasis, neuronal activity, mitosis, DNA repair and replication. Nuclear lncRNAs regulate transcription, organize subnuclear structure and mediate chromosomal interactions. In this case, NORAD function is still unknown (33,34). When an intense signal is detected in the nucleus, it may represent a site of transcription. Of note, no differences in NORAD levels were observed between normal and malignant cell lines. MCF-10A cell line just seems to express more of this lncRNA because it presents higher volume of cytoplasm, and MDA-MB-468 cell line shrinks during processing (Figure 4.2). To achieve this result, are required the optimization of the smRNA FISH protocol for cells to maintain their morphology, and the utilization of a quantitative method.

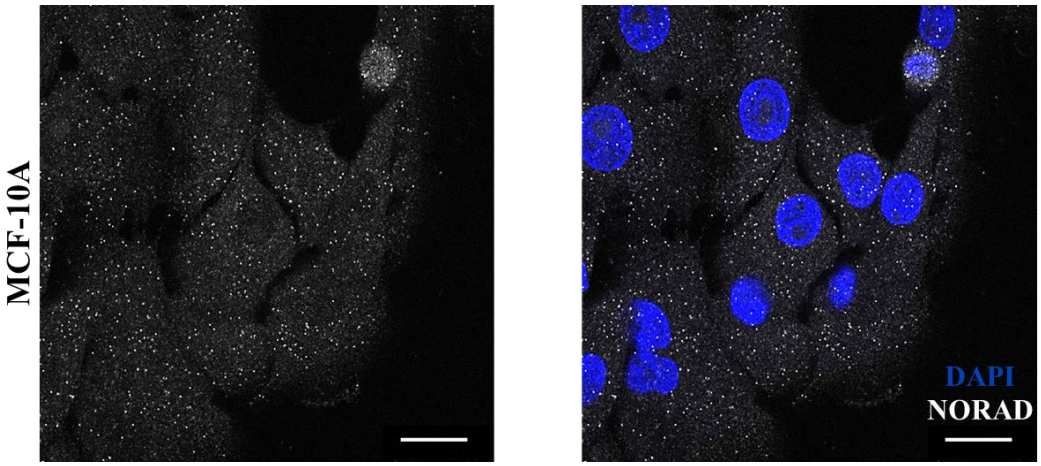

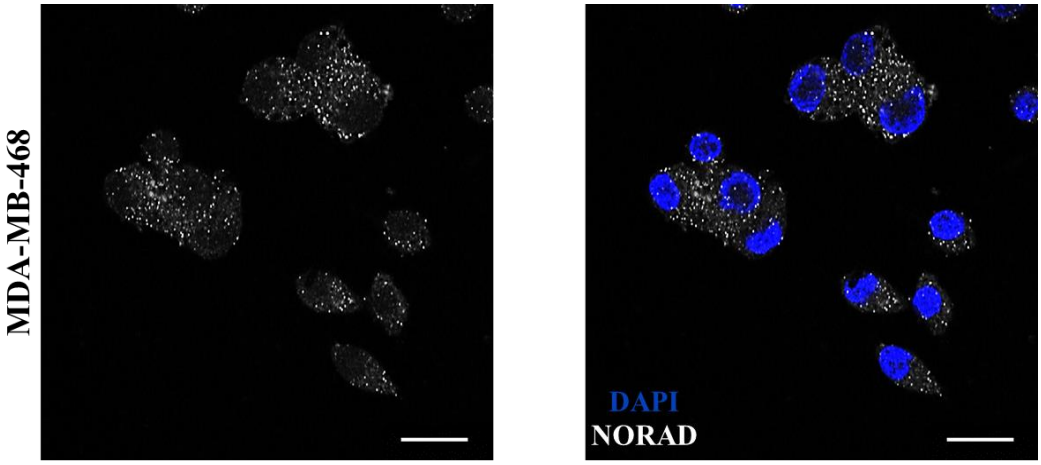

Figure 4.2: NORAD subcellular localization. smRNA FISH was performed in MCF-10A and MDA-MB-468 cell lines. Scale bar: 20µm.

4.3 NORAD knockdown optimization protocol

Next, the protocol for NORAD knockdown was optimized, using the MDA-MB-468 cell line, since its expression levels were significantly higher. Of note, knockdown efficiency is influenced by cells confluence since a high number of cells results in insufficient oligonucleotides, and a low number of cells results in cytotoxicity. First, two LNA™ GapmeRs that target different regions of NORAD were tested in comparison to a LNA™ GapmeR directed to a random sequence, at the final concentration of 50nM. At day one, cells were plated and transfected; 24h after, cells were transfected once again. Through RT-qPCR, was observed a reduction in NORAD levels for LNA™ GapmeR 1 but not for LNA™ GapmeR 3, and no differences were observed in the levels of p53 (Figure 7.1). Second, a combination of the two LNA™ GapmeRs was tested, at the final concentrations of 25nM and 50nM. At day one, cells were plated and transfected; 24h (Figure 7.2) or 48h (Figure 7.3) after, cells were transfected once again. Through RT-qPCR, no differences were observed in NORAD levels but was observed an increase in p53 levels, when the second transfection was performed 24h after the first transfection (Figure 7.2). In contrast, was observed a reduction in NORAD levels, when the second transfection was performed 48h after the first transfection (Figure 7.3). These results were obtained using β-actin as housekeeping gene. However, the knockdown efficiency was greater (more than 50%) when using 18S rRNA as housekeeping gene, both for 24h and 48h interval between transfections (Figure 7.4). The differences observed between these two housekeeping genes might be explained by the influence of treatments in their expression levels. Usually, 18S rRNA is more stable but both were validated as control genes for RT-qPCR analysis of human breast cancer cell lines containing different subtypes, using four different mathematical approaches (69). These results suggest that the combination of the two LNA™ GapmeRs improves the likelihood of RNase H-mediated cleavage. Despite LNA™ GapmeRs act mainly in the nucleus, they also have some activity in the cytoplasm (51). The increase in p53 levels might be a mechanism to compensate the chromosomal instability generated upon NORAD inactivation, subsequent PUMILIO hyperactivation and excessive repression of target mRNAs involved in mitosis, DNA repair and replication. However, Chen and colleagues found in germ cells that eight mRNAs encoding activators of p53 are repressed by Pumilio 1 (70). In addition, Hu and colleagues found in hepatocellular carcinoma that NORAD may function as a competitive endogenous RNA (ceRNA) in relation to miR-106a-5p, improving PTEN expression, which binds to p53 and triggers a conformational change that prevents MDM2-mediated degradation. PTEN also regulates p53 transcriptional activity by modulating its DNA binding. Loss of PTEN, induces AKT to bind to MDM2 and to phosphorylate it on serine residues, causing MDM2 nuclear translocation and p53 degradation (42,71). On the other hand, Li and colleagues found in pancreatic cancer that NORAD may also function

as a ceRNA in relation to hsa-miR-125a-3p, which could induce apoptosis via the p53 pathway in lung cancer (40). It is important to know if these are general mechanisms or cell type/cancer type-specific.

Third, a pool of four siRNAs that target different regions of NORAD (previously used by Tichon and colleagues) was tested, at the final concentrations of 12.5nM and 25nM, alone or in combination with LNA™ GapmeRs at the final concentration of 25nM, in comparison to a siRNA directed to a random sequence, at the final concentration of 25nM (34). This decision was related to the fact that siRNAs act mainly in the cytoplasm (51). At day one, cells were plated and transfected; 48h after, cells were transfected once again. Through RT-qPCR, was observed a reduction in NORAD levels, especially when cells were transfected with a combination of LNA™ GapmeRs and siRNAs (approximately 50%). In fact, since LNA™ GapmeRs and siRNAs show maximal activity in different compartments, combining them should lead to a stronger knockdown comparing to the single strategy (Figure 4.3) (51). Based on these results, was decided to perform NORAD knockdown using a combination of LNA™ GapmeRs and siRNAs, at a final concentration of 25nM, and with an interval of 48h between transfections. NORAD knockdown was confirmed by smRNA FISH in MDA-MB-468 and MCF-10A cell lines, where was observed a reduction in the amount of signal detected (Figures 4.4 and 7.5). In previous studies were also used shRNAs, transcription activator-like effector nucleases (TALENs) and clustered regulatory interspaced short palindromic repeats (CRISPR) – associated endonuclease 9 (Cas9) (33,34,38,42). LNA™ GapmeRs share some limitations with siRNAs: inefficient delivery, incomplete knockdown, off-target effects and temporary inhibition. On the other hand, genome-editing methods, such as TALENs and CRISPR/Cas9, could be effective for stable knockdown of lncRNAs but could not be translated to the clinic (43).

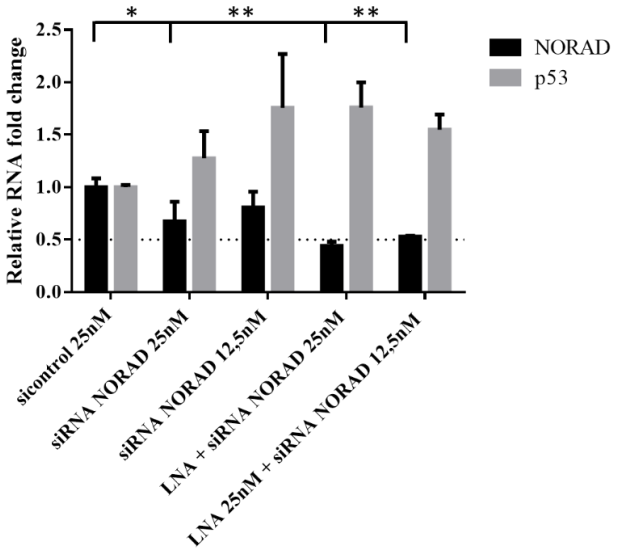

Figure 4.3: NORAD and p53 mRNA levels after NORAD knockdown, using LNA™ GapmeRs and siRNAs, with 48h interval between transfections. A pool of four siRNAs against NORAD was used at the final concentrations of 12.5nM and 25nM, alone or in combination with LNA™ GapmeRs at the final concentration of 25nM, in comparison to a non-specific siRNA at the final concentration of 25nM. RT-qPCR was performed in the MDA-MB-468 cell line, using pair of primers NORAD1 for the gene of interest and 18S rRNA as housekeeping gene. For statistical analysis was used one-way ANOVA, with the condition sicontrol 25nM for comparison. No-symbol $p>0.05$,* $p<0.05$, ** $p<0.01$.

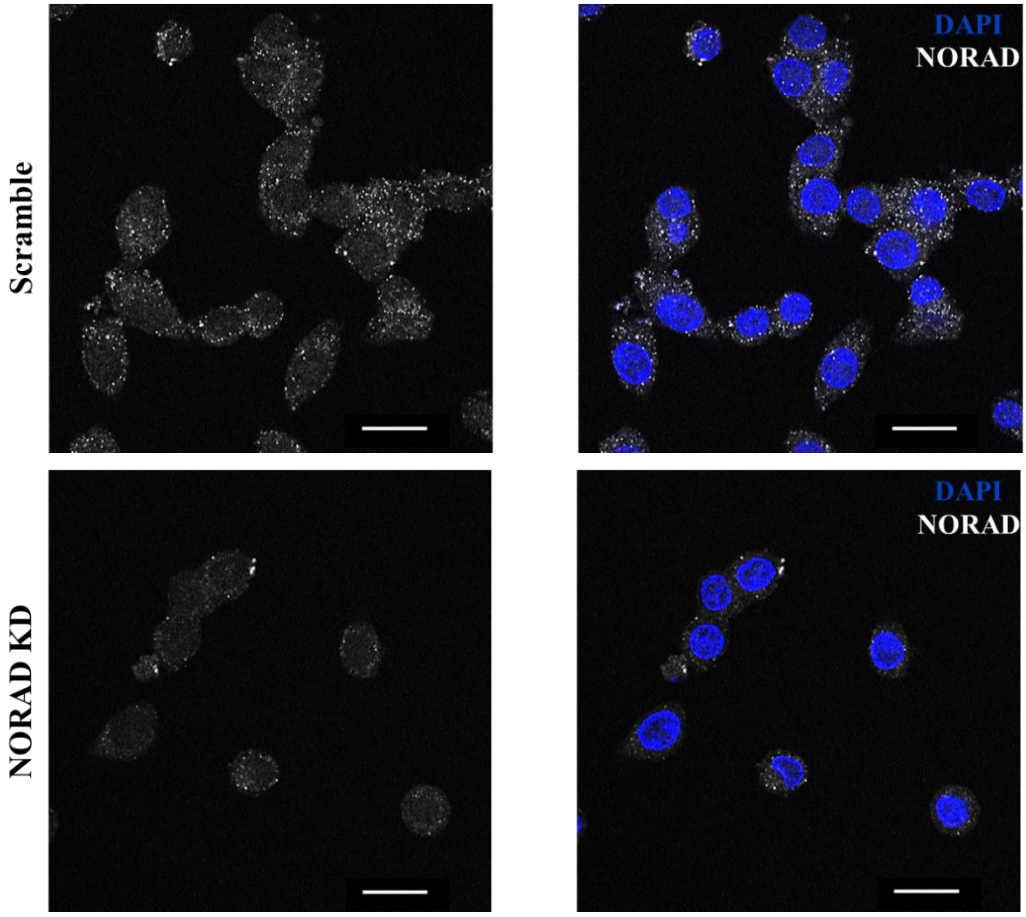

Figure 4.4: NORAD transcripts after knockdown I. smRNA FISH was performed in the MDA-MB-468 cell line. Scale bar: 20μm.

Tumor-relevant phenotypes were evaluated 48h after NORAD downregulation since it was previously demonstrated in U2OS cells that Pumilio target mRNAs were not substantially affected 24h after NORAD downregulation or overexpression (34).

4.4 NORAD knockdown inhibits cell proliferation

AlamarBlue® reduction assay was performed for the MDA-MB-468 cell line but no differences were observed in cell viability in comparison to the untreated condition or transfection with non-specific LNA™ GapmeR and siRNA. However, for the MDA-MB-231 cell line was observed a reduction in cell viability. Sustaining proliferative signaling is a hallmark of cancer, so this result suggests that this lncRNA may have a critical role in tumorigenesis (Figure 4.5). In fact, it was previously described that NORAD knockout by CRISPR/Cas9 in LM-4142, a derivative cell line from MDA-MB-231, caused significant reduction of cell viability (MTT assay) and number of colonies (clonogenic assay) (38). In contrast, NORAD knockdown by RNAi in hepatocellular carcinoma, promoted cell proliferation *in vitro* (CCK-8 and colony-formation assays) and tumor growth *in vivo* (42). A possible explanation for the contradictory results between MDA-MB-468 and 231 cell lines is that since the MDA-MB-468 cell line has lower expression of p53, cell cycle checkpoints are compromised and the cells continue to divide despite the chromosomal instability generated by NORAD downregulation. On the other hand, the MDA-MB-231 cell line has higher expression of p53, which induces cell cycle arrest or apoptosis (Figure 4.5).

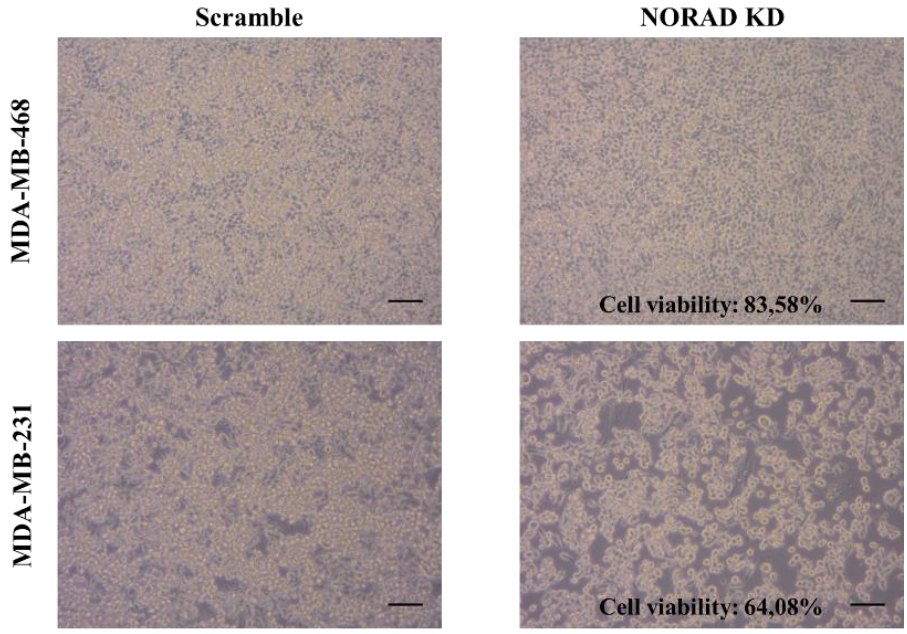

Figure 4.5: NORAD knockdown effect on cell viability. MDA-MB-468 and 231 cell lines were visualized and photographed in a Primo Vert inverted microscope (Carl Zeiss) (10x objective) incorporated with an AxioCam ER c5s. Scale bar: 100µm.

4.5 NORAD knockdown inhibits cell migration

The effect of NORAD was further characterized in the MDA-MB-231 cell line by the wound healing assay. At the time point 15h, it was already evident that the migration rate was lower after NORAD downregulation. Activating invasion and metastasis is another hallmark of cancer, so this result also supports the idea that NORAD may have a critical role in tumorigenesis (Figure 4.6). In fact, Li and colleagues have previously realized wound healing, transwell migration and invasion assays *in vitro* and *in vivo* for pancreatic cancer and obtained similar results. Of note, mice with NORAD downregulation presented more metastasis, including more distant metastasis (40). Hu and colleagues realized transwell chamber detection assay *in vitro* for hepatocellular carcinoma and obtained contradictory results since silencing of NORAD in Huh7 cells downregulated E-cadherin and ZO-1, while upregulated N-cadherin and slug (EMT-related factors), mediating cell migration and invasion (42).

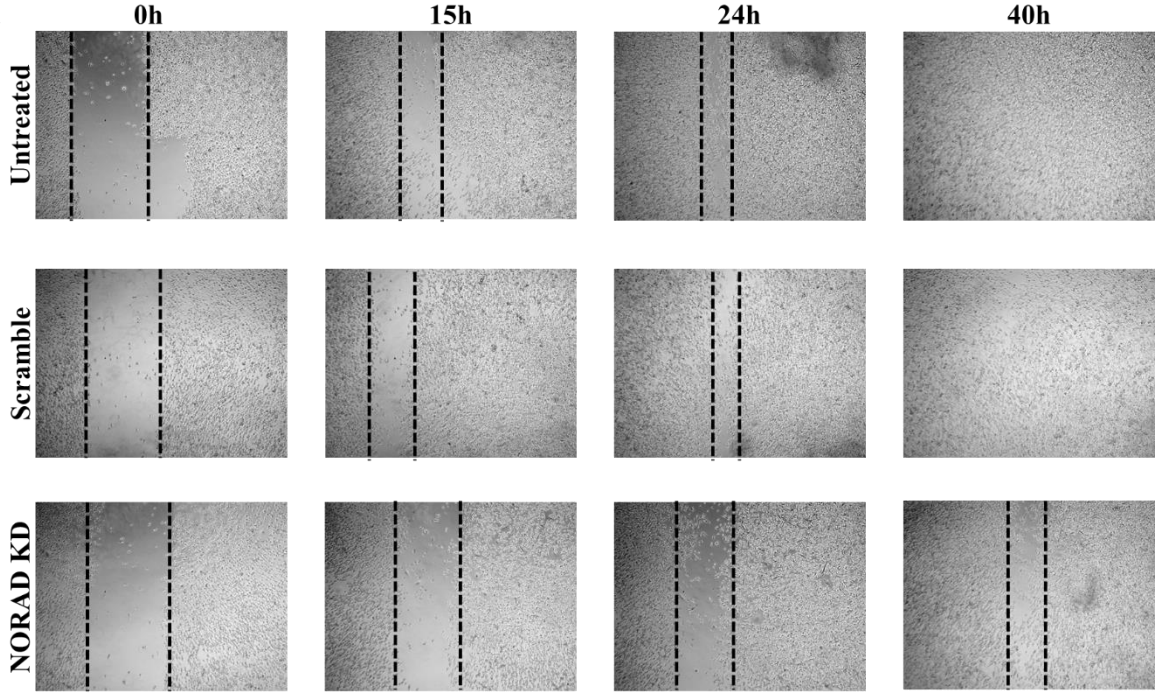

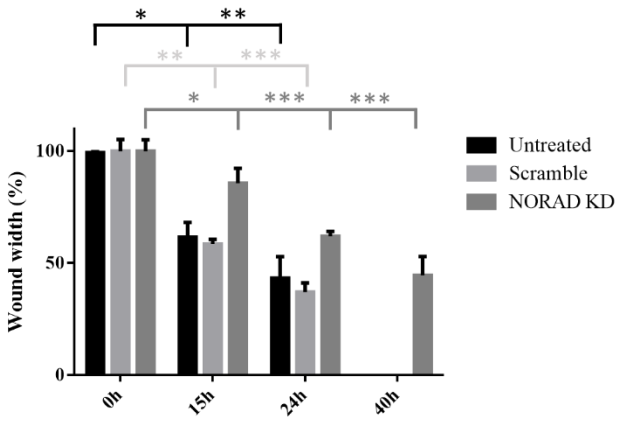

Figure 4.6: NORAD knockdown effect on cell migration. Wound healing assay was performed in the MDA-MB-231 cell line. For statistical analysis was used one-way ANOVA, with the time point 0h for comparison. No-symbol $p>0.05$, * $p<0.05$, ** $p<0.01$, ***$p<0.001$.

4.6 NORAD knockdown sensitizes breast cancer cells to chemotherapy

Chemotherapy is one of the therapies of choice for the treatment of cancer but its effectiveness is limited by resistance (35). P53 status influences the response to DNA damaging agents such as anthracyclines. Normal p53 may either induce apoptosis and tumor regression or cell cycle arrest and tumor resistance. Abnormal p53 may lead to accumulation of genetic abnormalities, either conferring tumor growth advantage through aneuploidy or inducing tumor regression through mitotic catastrophe (72). Since doxorubicin is one of the most common drugs used in the treatment of breast cancer, its IC_{50} was determined for MDA-MB-231 (IC_{50} = 1.252 µM) and MCF-10A cell lines (IC_{50} = 2.056 µM) (73). This value was higher for the non-malignant human mammary epithelial cell line because of chemotherapy selectivity towards cancer cells, which have higher proliferation rates. Moreover, normal p53 induces repair of DNA damage caused by doxorubicin in MCF-10A cells (Figure 7.6). Then, for the first time, the effects of combining NORAD knockdown with doxorubicin were evaluated. It was observed that NORAD knockdown sensitizes breast cancer cells to chemotherapy (IC_{50} shift from 0.3779 µM to 0.05680 µM) (Figure 4.7).

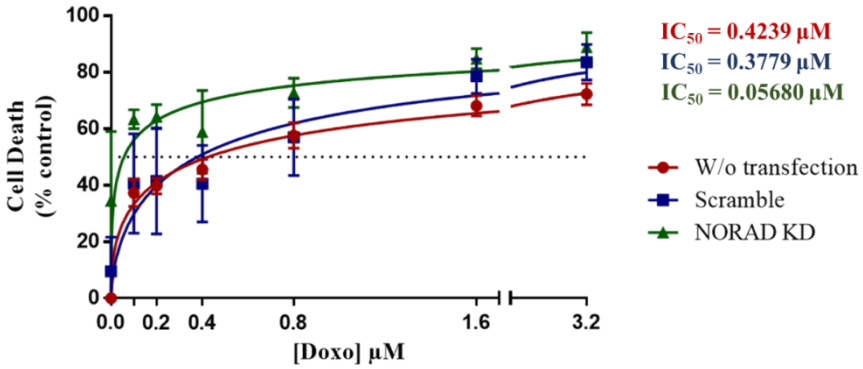

Figure 4.7: Effect of NORAD knockdown combination with chemotherapy. AlamarBlue® reduction assay was performed and doxorubicin IC_{50} was determined for the MDA-MB-231 cell line, in three different conditions: without transfection, transfection with non-specific LNA™ GapmeRs and siRNAs or against NORAD.

To better understand these results, mRNA levels of NORAD and p53 were determined by RT-qPCR for NORAD knockdown and/or incubation with doxorubicin (0.1 – 0.3µM). For NORAD knockdown was observed a decrease in NORAD levels and an increase in p53 levels induced by chromosomal instability (as already seen in the MDA-MB-468 cell line); for incubation with doxorubicin was observed an increase in NORAD and p53 levels induced by DNA damage as previously described by Lee and colleagues (33); for their combination was observed a decrease in NORAD levels and an increase in p53 levels (Figure 4.8).

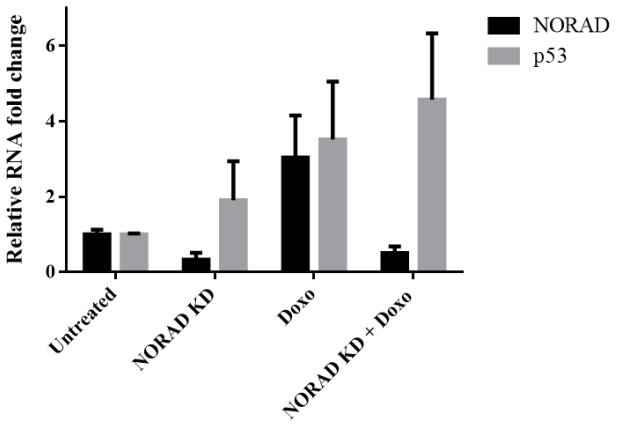

Figure 4.8: NORAD and p53 mRNA levels after NORAD knockdown and/or incubation with doxorubicin. RT-qPCR was performed in the MDA-MB-231 cell line, using pair of primers NORAD3 for the gene of interest and 18S rRNA as housekeeping gene. Doxorubicin was used at the final concentration of 0.1 – 0.3μM. For statistical analysis was used one-way ANOVA, with the condition untreated for comparison. No-symbol p>0.05.

Zhou and colleagues have previously highlighted the importance of CIN in drug resistance by demonstrating that the overexpression of CIN genes (involved in maintaining the genomic integrity of the cell) was associated with poor survival in myeloma and other cancers (74). However, at a certain time point, the accumulation of genetic abnormalities induced by the DNA damaging agent, NORAD knockdown and p53 deficiency is so high that results in cell death (25,72). The cell death observed with non-specific LNA™ GapmeR and siRNA corresponds to the inherent transfection cytotoxicity (Figure 4.7).

Protein levels of p53 and H2AX were also determined by western blot for the same conditions. For p53 was observed a significant increase in the presence of doxorubicin alone and in combination with knockdown of NORAD, which is consistent with our previous findings of mRNA levels by RT-qPCR (Figure 4.9).

The histone variant H2AX represents 2.5 – 25% of H2A protein family, which is a component of the histone octomer in nucleosomes (75,76). Immediately after DNA double-strand break, H2AX is phosphorylated (γH2AX) mainly by ATM at C-terminal Ser136 and Ser139 residues, recruits MDC1, which in turn recruits Mre11-Rad50-Nbs1 complex. This results in further activation of ATM, spread of H2AX phosphorylation, chromatin remodeling and recruitment of components of DNA repair, including BRCA1 and 53BP1. After DNA repair, H2AX is dephosphorylated by PP2A (75–77). In addition to phosphorylation, ubiquitination of H2AX is an important epigenetic marker for DNA lesions in DNA damage response. Monoubiquitination of H2AX at Lys-119/Lys-120 mediated by the RNF2-BMI1 complex, leads to the recruitment of active ATM, phosphorylation of H2AX, recruitment of MDC1 and other DNA repair proteins. RNF2 and BMI1 are RING-domain containing proteins that are part of the polycomb repressive complex 1, and are important for transcriptional silencing of regions around the damage (78,79). Alternatively, may be considered the RING-type ubiquitin E3 ligases, RNF8 and RNF168. Once RNF8 accumulates at the lesions, it forms free ubiquitin chains or ubiquitin chains attached to proteins localized in the proximity. This results in RNF168 recruitment, which is responsible for H2AX ubiquitination on K13-15, where K63 chains are extended by RNF8. This signal not only allows the recruitment of downstream proteins of the double-strand break cascade, such as 53BP1 and BRCA1, but also induces nucleosomal rearrangements that are important during the assembly of the repair machinery (80). An obvious advantage of γH2AX compared to other DNA damage markers is its extremely high sensitivity that enables detection of very small changes in genome integrity on a single cell level (81).

In the present study, H2AX was detected in the presence of doxorubicin alone that causes double-strand breaks, which suggests recruitment of DNA repair proteins. Despite the antibody used is specific to γH2AX, it also recognized what we believe to be the ubiquitylated form, based on what is described for identical antibodies (ab11174). However, an antibody specific to Ub-γH2AX would be required to confirm this hypothesis. Surprisingly, the signal almost disappeared in the combination of doxorubicin with NORAD knockdown, which causes DNA damage and chromosomal instability. These data could be explained by DNA repair as suggested by RT-qPCR results, where p53 levels are higher in the combination of doxorubicin with NORAD knockdown. This could also be true for other checkpoint proteins and would require cell cycle arrest. Another possible explanation could be cell death. Despite some studies report that cell death-associated DNA fragmentation also leads to phosphorylation of H2AX, this occurs especially long time periods after drug treatment or in case of agents that induce rapid apoptosis (Figure 4.9) (81). To confirm these results, western blot should be repeated with a precise method of protein quantification instead of Coomassie blue staining, such as Bradford or BCA (bicinchoninic acid) protein assay. In fact, the condition of NORAD knockdown alone could not be considered since expression level of the housekeeping gene is different. Moreover, instead of western blot, could be performed the comet assay consisting of individual cells with damaged DNA embedded in agarose gels that are subjected to an electric field and generate a characteristic pattern of DNA distribution forming a tail that, after staining with a fluorescence dye, can be analyzed by fluorescence microscopy. The extent and length of the comet's tail correlates with the severity of DNA damage. However, the sensitivity of the comet assay depends on proper calibration and its specificity is not absolute. Alternatively, immunocytochemistry offers much greater sensitivity, since it allows detection of γH2AX in chromatin, in the form of discrete nuclear foci, with each focus representing a single double-strand break (81).

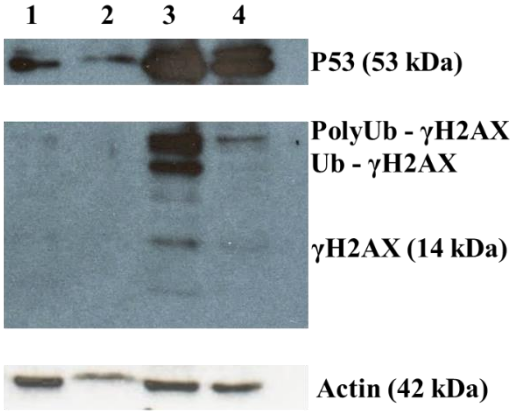

Figure 4.9: p53 and γH2AX protein levels after NORAD knockdown and/or incubation with doxorubicin. Western blot was performed in the MDA-MB-231 cell line, using β-actin as housekeeping protein. Conditions: 1 - Untreated, 2 - NORAD knockdown, 3 – Doxorubicin (0.1 – 0.3μM) and 4 - NORAD knockdown + doxorubicin.

4.7 NORAD knockdown promotes cell death

To understand the nature of the sensitization to doxorubicin, cell apoptosis was determined. While for NORAD inactivation no differences were observed in comparison to negative controls, in combination with doxorubicin (0.1 – 0.3μM) was observed an increase in apoptosis, which was consistent with our previous findings (Figure 4.10). Despite the p53 mutation in MDA-MB-231 cells, redundant mechanisms may compensate for it. For example, in Saos-2 cells (osteosarcoma), doxorubicin was able to increase intracellular peroxide levels, which mediate mitochondrial membrane depolarization, mitochondrial cytochrome c release, cytosolic caspase-3 activation and, ultimately, apoptosis (82). However, the optimization of this protocol is required, so that the differences become more evident. Despite the effect on cell metabolism was detected 48h after doxorubicin treatment by the alamarBlue® reduction assay, the cell death is not induced in the short term because the deleterious

effects of severe chromosome mis-segregations are not expected to become apparent before 2-6 divisions have occurred. In a study performed by Janssen and colleagues, the effect on cell viability (U2OS, HCT-116, LS174 and HeLa) was determined 4-11 days after taxol treatment (25). Dose and incubation time with the drug should also be considered. On the other hand, since the MDA-MB-231 cell line presents a p53 mutation and, consequently, defective checkpoints, cell death can occur during mitosis (mitotic catastrophe), which is an apoptosis-independent event. Mitotic catastrophe is a result of centrosome overduplication and subsequent entry into mitosis with multiple spindle poles, which leads to the formation of giant micronucleated cells and subsequent mechanical collapse, with no signs of DNA fragmentation (83).

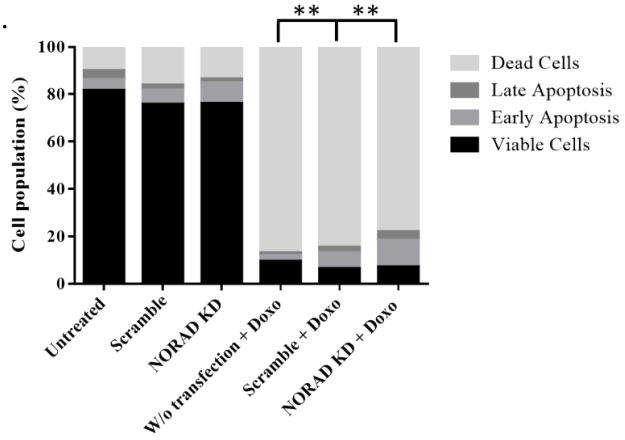

Figure 4.10: NORAD knockdown and doxorubicin effects on cell apoptosis. Cell apoptosis was analyzed by flow cytometry in the MDA-MB-231 cell line. Doxorubicin was used at the final concentration of 0.1 – 0.3μM. For statistical analysis was used one-way ANOVA, with the conditions untreated and w/o transfection + doxo for comparison. No-symbol $p>0.05$, ** $p<0.01$.

4.8 NORAD knockdown does not affect cell cycle

Cell cycle was also analyzed but no cell cycle arrest was observed upon NORAD inactivation, just an increase in the number of cells in S phase. Despite chromosomal instability, MDA-MB-231 cells continue to divide, more rapidly without G_1 or G_2 checkpoints, because they present a p53 mutation, and the accumulation of genetic abnormalities confers tumor growth advantage. In the presence of doxorubicin (0.1 – 0.3μM), was observed similar cell cycle arrest in G_2 phase for different conditions, indicating that this lncRNA is not required for these aspects of the DNA damage response, as already described by Lee and colleagues (Figure 4.11) (33). Siu and colleagues have demonstrated that doxorubicin is capable of inducing G_1 cell cycle arrest, which correlated with the activation of p53 and $p21^{Cip1/Waf1}$. In G_0 phase, doxorubicin caused a prolonged cell cycle arrest, while in G_0-G_1 transition or G_1 phase, doxorubicin caused only a transient cell cycle delay. In contrast, doxorubicin-induced G_2 cell cycle arrest was more permanent and correlated with the Thr-14/Tyr-15 phosphorylation of cyclin B-Cdc2 complexes. Therefore, cells that initially arrested in G_1 phase may eventually accumulate in G_2 phase (84). Of note, Shin and colleagues have demonstrated that doxorubicin activity is p53-independent (85).

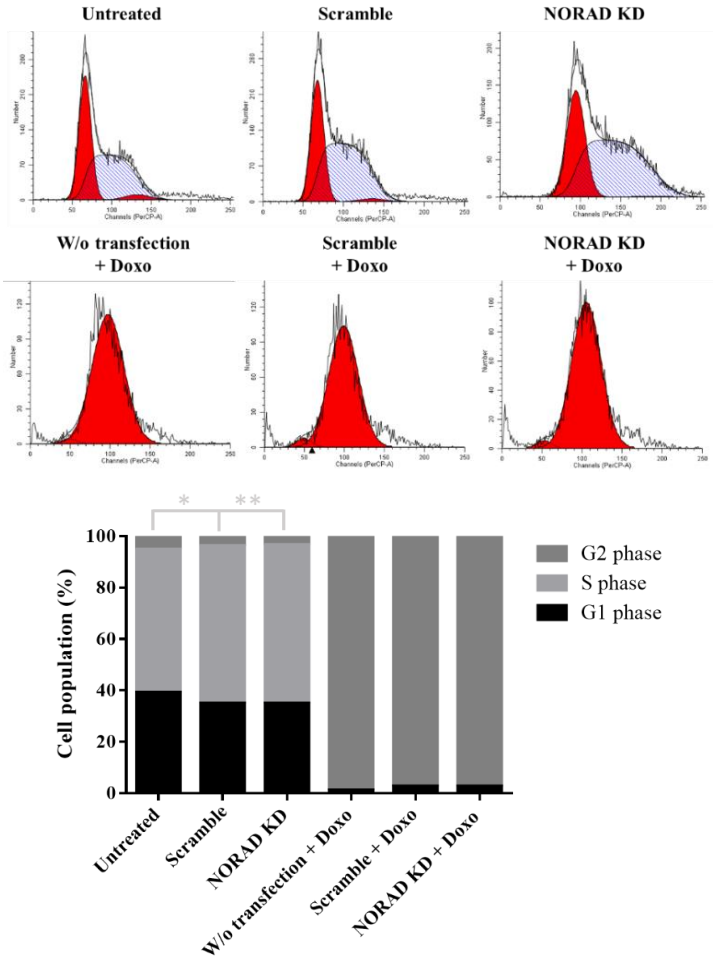

Figure 4.11: NORAD knockdown and doxorubicin effects on cell cycle. Cell cycle was analyzed by flow cytometry in the MDA-MB-231 cell line. Doxorubicin was used at the final concentration of 0.1 – 0.3μM. For statistical analysis was used one-way ANOVA, with the conditions untreated and w/o transfection + doxo for comparison. No-symbol $p>0.05$, * $p<0.05$, ** $p<0.01$.

4.9 Correlation between NORAD expression and survival of breast cancer patients

Finally, the Kaplan-Meier Plotter, a tool whose primary purpose is a meta-analysis based biomarker assessment, was used to assess the effect of NORAD expression on overall survival and relapse-free survival of breast cancer patients (86). Considering all breast cancer subtypes at the same cluster, NORAD expression does not influence these two parameters. However, considering each subtype individually, only for basal-like tumors was observed a negative correlation between expression of NORAD and relapse-free survival but not overall survival. The other breast cancer subtypes mask the result observed for basal-like tumors, which are the most aggressive. Therefore, this lncRNA may represent a tumor marker for patient prognosis (Figure 4.12). This association of NORAD upregulation with poor prognosis was previously observed for breast cancer, esophageal squamous cell carcinoma and pancreatic cancer, while the opposite was observed for hepatocellular carcinoma (38–40,42).

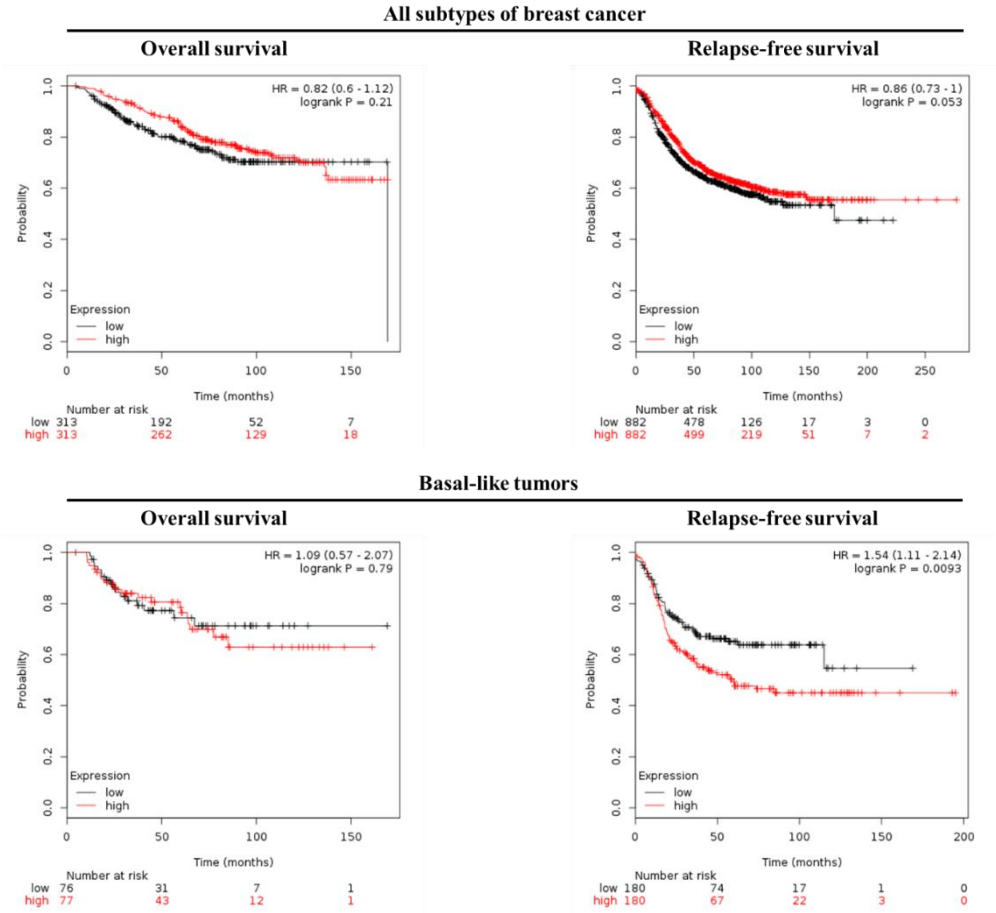

Figure 4.12: Breast cancer patients overall survival and relapse-free survival according to NORAD expression levels. Graphs were obtained with Kaplan-Meier Plotter. All subtypes (OS: n=626, RFS: n=1764). Basal-like tumors (OS: n=153, RFS: n=360). HR: hazard ratio. CI: 95% confidence interval.

5. Conclusions and future perspectives

Here we report that the lncRNA NORAD expression is upregulated in breast cancer cells, and that its knockdown inhibits cell proliferation, migration and promotes cell death, sensitizing breast cancer cells to chemotherapy. In fact, chromosomal instability generated upon NORAD downregulation, in combination with DNA damage induced by doxorubicin, is known to result in severe chromosome mis-segregations incompatible with cell viability. We also highlight p53 as the guardian of the genome in these stress conditions since its expression levels increase. Therefore, this lncRNA may represent a tumor marker for disease diagnosis, patient prognosis or therapy response, and may represent a therapeutic target, at least in breast cancer. However, molecular heterogeneity of breast cancer, dual action of NORAD as an oncogene and tumor suppressor gene, and contradictory results in different types of cancer, argue for a need of more studies to fully assess its role.

It would be of great interest to investigate how MCF-7 cell line responds to NORAD knockdown and DNA damage since it differs from MDA-MB-231 cell line in some aspects: belongs to the luminal subtype and presents wild-type p53 and mutant BRCA1 gene sequence (which plays an important role in the maintenance of genomic integrity, interacting with various DNA damage repair proteins like MSH2, RAD51, ATM, BLM and RAD50-MRE11-NBS1) (87).

It would also be interesting to test the same cell lines in the presence of the chemotherapeutic agent taxol (generic name paclitaxel), since its mode of action is distinct. It binds to a subunit of tubulin heterodimer, accelerating the polymerization of tubulin and inhibiting the depolymerization of microtubules (88). Chromatids connect to spindle microtubules through kinetochores, protein complexes that assemble on centromeric regions of DNA. Taxol treatment reduces the tension on

kinetochores that maintain bipolar attachment, which results in a small number of unattached kinetochores, activation of the spindle assembly checkpoint, arrest of cells in metaphase and, ultimately, apoptosis (89).

Once we verified a shift of doxorubicin IC_{50} in MDA-MB-231 cell line upon NORAD knockdown, we intend to develop a cell line resistant to this chemotherapeutic agent by incubation with gradually higher doses until no cell death is observed, in order to evaluate if we are able to achieve the same result.

We also intend to analyze NORAD expression levels in breast tumor tissues from patients in comparison to the corresponding normal tissues by RT-qPCR and smRNA FISH, and to correlate higher expression levels of NORAD with specific tissue structures associated with malignancy (for example, more vasculature) by hematoxylin and eosin staining and smRNA FISH, in order to evaluate if the results are consistent with those obtained for the epithelial breast cancer cell lines, and confirm if this lncRNA may function as a tumor marker for disease diagnosis, patient prognosis and therapy response.

Finally, we plan to employ CRISPR-Cas9 for stable NORAD knockdown to fully confirm our results; and to perform NORAD overexpression in the non-malignant human mammary epithelial cell line MCF-10A to see if NORAD alone could lead to oncogenic transformation. This would be an irrefutable proof of this lncRNA critical role in tumorigenesis.

6. References

1. Hanahan D, Weinberg RA. The hallmarks of cancer. Cell. 2000;100(1):57–70.
2. Hanahan D, Weinberg RA. Hallmarks of cancer: The next generation. Cell. 2011;144(5):646–74.
3. Lee EYHP, Muller WJ. Oncogenes and Tumor Suppressor Genes. Cold Spring Harb Perspect Biol. 2010;2(10).
4. Wieman HL, Wofford JA, Rathmell JC. Cytokine stimulation promotes glucose uptake via phosphatidylinositol-3 kinase/Akt regulation of Glut1 activity and trafficking. Mol Biol Cell. 2007;18(4):1437–1446.
5. Chavez KJ, Garimella S V., Lipkowitz S. Triple Negative Breast Cancer Cell Lines: One Tool in the Search for Better Treatment of Triple Negative Breast Cancer. Breast Dis. 2010;32(1–2):35–48.
6. Ismail-Khan R, Bui MM. A review of triple-negative breast cancer. Cancer Control. 2010;17(3):173–6.
7. American Cancer Society. Cancer Facts and Figures 2017. 2017
8. Yates LR, Knappskog S, Wedge D, Farmery JHR, Gonzalez S, Martincorena I, et al. Genomic Evolution of Breast Cancer Metastasis and Relapse. Cancer Cell. 2017;32(2):169–84.
9. Holliday DL, Speirs V. Choosing the right cell line for breast cancer research. Breast cancer Res. 2011;13(4):215.
10. Brenton JD, Carey LA, Ahmed A, Caldas C. Molecular classification and molecular forecasting of breast cancer: Ready for clinical application? J Clin Oncol. 2005;23(29):7350–60.
11. Kwei K, Kung Y, Salari K, Holcomb I, Pollack JR. Genomic instability in breast cancer: pathogenesis and clinical implications. Mol Oncol. 2010;4(3):255–66.
12. Toss A, Cristofanilli M. Molecular characterization and targeted therapeutic approaches in breast cancer. Breast Cancer Res. 2015;17:60.
13. Bertheau P, Lehmann-Che J, Varna M, Dumay A, Poirot B, Porcher R, et al. P53 in breast cancer subtypes and new insights into response to chemotherapy. Breast. 2013;22(Suppl 2):S27–9.
14. National Cancer Institute. Available from: https://www.cancer.gov/
15. Anders CK, Carey LA. Biology, Metastatic Patterns and Treatment of Patients with Triple-Negtive Breast Cancer. Clin Breast Cancer. 2009;9(Suppl 2):S73–81.
16. Palma G, Frasci G, Chirico A, Esposito E, Siani C, Saturnino C, et al. Triple negative breast cancer: looking for the missing link between biology and treatments. Oncotarget. 2015;6(29):26560–74.
17. European Medicines Agency. Available from: http://www.ema.europa.eu/ema/
18. Cancer Research UK. Available from: https://www.cancerresearchuk.org/
19. Chemocare. Available from: http://www.chemocare.com/
20. DrugBank. Available from: https://www.drugbank.ca/
21. Jackson SP, Bartek J. The DNA-damage response in human biology and disease. Nature. 2009;461(7267):1071–8.
22. Ciccia A, Elledge SJ. The DNA Damage Response: Making It Safe to Play with Knives. Mol Cell. 2010;40(2):179–204.
23. Lodish H, Berk A, Kaiser CA, Krieger M, Bretscher A, Ploegh H, et al. Molecular Cell Biology. 7th ed.

McHenry B, Tontonoz M, Frost EP, Champion E, Rolfes M, Byrd ML, et al., editors. W. H. Freeman and Company. New York: Katherine Ahr Parker; 2013. 1113-1148 p.
24. Kastan MB, Onyekwere O, Sidransky D, Vogelstein B, Craig RW. Participation of p53 Protein in the Cellular Response to DNA Damage. Cancer Res. 1991;51(23 Pt 1):6304–11.
25. Janssen A, Kops GJPL, Medema RH. Elevating the frequency of chromosome mis-segregation as a strategy to kill tumor cells. PNAS. 2009;106(45):19108–13.
26. Bouwman P, Jonkers J. The effects of deregulated DNA damage signalling on cancer chemotherapy response and resistance. Nat Rev Cancer. 2012;12(9):587–98.
27. Lane DP. p53, guardian of the genome. Nature. 1992;358(6381):15–6.
28. Lowe SW, Cepero E, Evan G. Intrinsic tumour suppression. Nature. 2004;432(7015):307–15.
29. Schwartz D, Rotter V. P53-Dependent Cell Cycle Control: Response To Genotoxic Stress. Semin Cancer Biol. 1998;8(5):325–36.
30. Junttila MR, Evan GI. P53 - a Jack of all trades but master of none. Nat Rev Cancer. 2009;9(11):821–9.
31. Kastenhuber ER, Lowe SW. Putting p53 in Context. Cell. 2017;170(6):1062–78.
32. Silwal-Pandit L, Vollan HKM, Chin SF, Rueda OM, McKinney S, Osako T, et al. TP53 mutation spectrum in breast cancer is subtype specific and has distinct prognostic relevance. Clin Cancer Res. 2014;20(13):3569–80.
33. Lee S, Kopp F, Chang TC, Sataluri A, Chen B, Sivakumar S, et al. Noncoding RNA NORAD Regulates Genomic Stability by Sequestering PUMILIO Proteins. Cell. 2016;164(1–2):69–80.
34. Tichon A, Gil N, Lubelsky Y, Solomon TH, Lemze D, Itzkovitz S, et al. A conserved abundant cytoplasmic long noncoding RNA modulates repression by Pumilio proteins in human cells. Nat Commun. 2016;7:12209.
35. Holohan C, Van Schaeybroeck S, Longley DB, Johnston PG. Cancer drug resistance: An evolving paradigm. Nat Rev Cancer. 2013;13(10):714–26.
36. Guan X, Chen S, Liu Y, Wang L, Zhao Y, Zong Z-H. PUM1 promotes ovarian cancer proliferation, migration and invasion. Biochem Biophys Res Commun. 2018;(18):30301–2.
37. Tichon A, Perry RB, Stojic L, Ulitsky I. SAM68 is required for regulation of Pumilio by the NORAD long noncoding RNA. Genes Dev. 2018;32(1):70–8.
38. Liu H, Li J, Koirala P, Ding X, Chen B, Wang Y, et al. Long non-coding RNAs as prognostic markers in human breast cancer. Oncotarget. 2016;7(15):20584–96.
39. Wu X, Lim Z-F, Li Z, Gu L, Ma W, Zhou Q, et al. NORAD Expression Is Associated with Adverse Prognosis in Esophageal Squamous Cell Carcinoma. Oncol Res Treat. 2017;40(6):370–4.
40. Li H, Wang X, Wen C, Huo Z, Wang W, Zhan Q, et al. Long noncoding RNA NORAD, a novel competing endogenous RNA, enhances the hypoxia-induced epithelial-mesenchymal transition to promote metastasis in pancreatic cancer. Mol Cancer. 2017;16:169.
41. Bao M, Li G, Huang X, Tang L, Dong L, Li J. Long non-coding RNA LINC00657 acting as miR-590-3p sponge to facilitate low concentration oxidized low-density lipoprotein-induced angiogenesis. Mol Pharmacol. 2018;
42. Hu B, Cai H, Zheng R, Yang S, Zhou Z, Tu J. Long non-coding RNA 657 suppresses hepatocellular carcinoma cell growth by acting as a molecular sponge of miR-106a-5p to regulate PTEN expression. Int J Biochem Cell Biol. 2017;92:34–42.
43. Huarte M. The emerging role of lncRNAs in cancer. Nat Med. 2015;21(11):1253–61.
44. Gutschner T, Diederichs S. The hallmarks of cancer: A long non-coding RNA point of view. RNA Biol. 2012;9(6):703–19.
45. Ventura A. NORAD: Defender of the Genome. Trends Genet. 2016;32(7):390–2.
46. Schmitt AM, Chang HY. Long Noncoding RNAs in Cancer Pathways. Cancer Cell. 2016;29(4):452–63.
47. Djebali S, Davis CA, Merkel A, Dobin A, Lassmann T, Mortazavi A, et al. Landscape of transcription in human cells. Nature. 2012;489(7414):101–8.
48. Scitable. Available from: https://www.nature.com/scitable
49. Kung JTY, Colognori D, Lee JT. Long Noncoding RNAs: Past, Present, and Future. Genetics. 2013;193(3):651–69.
50. Dharmacon. Available from: http://dharmacon.gelifesciences.com/
51. Lennox KA, Behlke MA. Cellular localization of long non-coding RNAs affects silencing by RNAi more than by antisense oligonucleotides. Nucleic Acids Res. 2016;44(2):863–77.
52. Exiqon. Available from: http://www.exiqon.com/
53. Corrie PG. Cytotoxic chemotherapy: clinical aspects. Medicine. 2004;32(3):25–9.
54. Spänkuch B, Strebhardt K. Combinatorial Application of Nucleic Acid-Based Agents Targeting Protein Kinases for Cancer Treatment. Curr Pharm Des. 2008;14(11):1098–112.
55. Lind M. Principles of Cytotoxic Chemotherapy. Medicine. 2008;36(1):19–23.
56. PubChem. Available from: https://pubchem.ncbi.nlm.nih.gov/

57. Gewirtz DA. A critical evaluation of the mechanisms of action proposed for the antitumor effects of the anthracycline antibiotics adriamycin and daunorubicin. Biochem Pharmacol. 1999;57(7):727–41.
58. Denard B, Lee C, Ye J. Doxorubicin blocks proliferation of cancer cells through proteolytic activation of CREB3L1. Elife. 2012;1.
59. Patel AG, Kaufmann SH. How does doxorubicin work? Elife. 2012;1.
60. Denard B, Seemann J, Chen Q, Gay A, Huang H, Chen Y, et al. The membrane-bound transcription factor CREB3L1 is activated in response to virus infection to inhibit proliferation of virus-infected cells. Cell Host Microbe. 2011;10(1):65–74.
61. Malhotra V, Perry MC. Classical chemotherapy: mechanisms, toxicities and the therapeutic window. Cancer Biol Ther. 2003;2(4 Suppl 1):S2-4.
62. Melisi D, Troiani T, Damiano V, Tortora G, Ciardiello F. Therapeutic integration of signal transduction targeting agents and conventional anti-cancer treatments. Endocr Relat Cancer. 2004;11(1):51–68.
63. Biroccio A, Leonetti C, Zupi G. The future of antisense therapy: combination with anticancer treatments. Oncogene. 2003;22(42):6579–88.
64. Li P, Zhang X, Wang L, Du L, Yang Y, Liu T, et al. lncRNA HOTAIR Contributes to 5FU Resistance through Suppressing miR-218 and Activating NF-κB/TS Signaling in Colorectal Cancer. Mol Ther - Nucleic Acids. 2017;8:356–69.
65. Neve RM, Chin K, Fridlyand J, Yeh J, Baehner FL, Fevr T, et al. A collection of breast cancer cell lines for the study of functionally distinct cancer subtypes. Cancer Cell. 2006;10(6):515–27.
66. Hollestelle A, Nagel JHA, Smid M, Lam S, Elstrodt F, Wasielewski M, et al. Distinct gene mutation profiles among luminal-type and basal-type breast cancer cell lines. Breast Cancer Res Treat. 2010;121(1):53–64.
67. Iyer MK, Niknafs YS, Malik R, Singhal U, Sahu A, Hosono Y, et al. The Landscape of Long Noncoding RNAs in the Human Transcriptome. Nat Genet. 2015;47(3):199–208.
68. Sigal A, Rotter V. Oncogenic Mutations of the p53 Tumor Suppressor : The Demons of the Guardian of the Genome. Cancer Res. 2000;60(24):6788–93.
69. Liu LL, Zhao H, Ma TF, Ge F, Chen CS, Zhang YP. Identification of valid reference genes for the normalization of RT-qPCR expression studies in human breast cancer cell lines treated with and without transient transfection. PLoS One. 2015;10(1).
70. Chen D, Zheng W, Lin A, Uyhazi K, Zhao H, Lin H. Pumilio 1 suppresses multiple activators of p53 to safeguard spermatogenesis. Curr Biol. 2012;22(5):420–5.
71. Freeman DJ, Li AG, Wei G, Li H-H, Kertesz N, Lesche R, et al. PTEN tumor suppressor regulates p53 protein levels and activity through phosphatase-dependent and-independent mechanisms. Cancer Cell. 2003;3:117–30.
72. Bertheau P, Espié M, Turpin E, Lehmann J, Plassa LF, Varna M, et al. TP53 status and response to chemotherapy in breast cancer. Pathobiology. 2008;75(2):132–9.
73. American Cancer Society. Available from: https://www.cancer.org/
74. Zhou W, Yang Y, Xia J, Wang H, Salama ME, Xiong W, et al. NEK2 Induces Drug-resistance Mainly through Activation of Efflux Drug Pumps and Is Associated with Poor Prognosis in Myeloma and Other Cancers. Cancer Cell. 2013;23(1):48–62.
75. Kuo LJ, Yang L-X. γ-H2AX - a novel biomarker for DNA double-strand breaks. In Vivo. 2008;22(3):305–9.
76. Turinetto V, Giachino C. Multiple facets of histone variant H2AX: A DNA double-strand-break marker with several biological functions. Nucleic Acids Res. 2015;43(5):2489–98.
77. Kang J, Ferguson D, Song H, Bassing C, Eckersdorff M, Alt FW, et al. Functional Interaction of H2AX, NBS1, and p53 in ATM-Dependent DNA Damage Responses and Tumor Suppression. Mol Cell Biol. 2005;25(2):661–70.
78. Wu CY, Kang HY, Yang WL, Wu J, Jeong YS, Wang J, et al. Critical role of monoubiquitination of histone H2AX protein in histone H2AX phosphorylation and DNA damage response. J Biol Chem. 2011;286(35):30806–15.
79. Pan MR, Peng G, Hung W-C, Lin S-Y. Monoubiquitination of H2AX protein regulates DNA damage response signaling. J Biol Chem. 2011;286(32):28599–607.
80. Mattiroli F, Vissers JHA, Van Dijk WJ, Ikpa P, Citterio E, Vermeulen W, et al. RNF168 ubiquitinates K13-15 on H2A/H2AX to drive DNA damage signaling. Cell. 2012;150(6):1182–95.
81. Podhorecka M, Skladanowski A, Bozko P. H2AX Phosphorylation: Its Role in DNA Damage Response and Cancer Therapy. J Nucleic Acids. 2010;2010.
82. Tsang WP, Chau SPY, Kong SK, Fung KP, Kwok TT. Reactive oxygen species mediate doxorubicin induced p53-independent apoptosis. Life Sci. 2003;73(16):2047–58.
83. Fragkos M, Beard P. Mitotic catastrophe occurs in the absence of apoptosis in p53-null cells with a defective G1 checkpoint. PLoS One. 2011;6(8).

84. Siu WY, Yam CH, Poon RYC. G1 versus G2 cell cycle arrest after adriamycin-induced damage in mouse Swiss3T3 cells. FEBS Lett. 1999;461(3):299–305.
85. Shin HJ, Kwon HK, Lee JH, Gui X, Achek A, Kim JH, et al. Doxorubicin-induced necrosis is mediated by poly-(ADP-ribose) polymerase 1 (PARP1) but is independent of p53. Sci Rep. 2015;5.
86. Lánczky A, Nagy Á, Bottai G, Munkácsy G, Szabó A, Santarpia L, et al. miRpower: a web-tool to validate survival-associated miRNAs utilizing expression data from 2178 breast cancer patients. Breast Cancer Res Treat. 2016;160(3):439–46.
87. Francisco DC, Peddi P, Hair JM, Flood BA, Cecil AM, Kalogerinis PT, et al. Induction and processing of complex DNA damage in human breast cancer cells MCF-7 and nonmalignant MCF-10A cells. Free Radic Biol Med. 2008;44(4):558–69.
88. Spänkuch B, Heim S, Kurunci-Csacsko E, Lindenau C, Yuan J, Kaufmann M, et al. Down-regulation of polo-like kinase 1 elevates drug sensitivity of breast cancer cells in vitro and in vivo. Cancer Res. 2006;66(11):5836–46.
89. Weaver BA. How Taxol/paclitaxel kills cancer cells. Mol Biol Cell. 2014;25(18):2677–81.

7. Supplementary figures

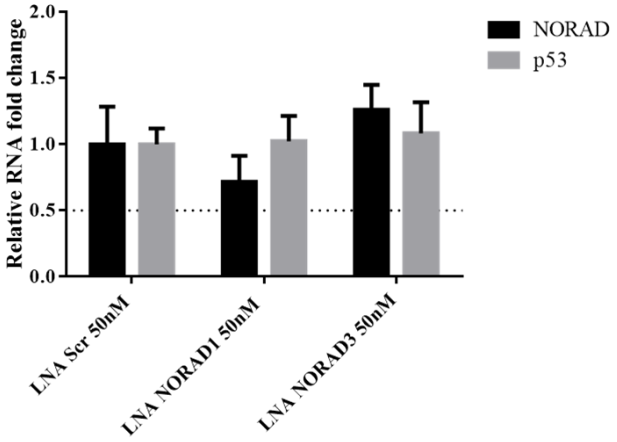

Figure 7.1: NORAD and p53 mRNA levels after NORAD knockdown, using LNA™ GapmeRs, with 24h interval between transfections. Two LNA™ GapmeRs against NORAD were tested in comparison to a non-specific LNA™ GapmeR, at the final concentration of 50nM. RT-qPCR was performed in the MDA-MB-468 cell line, using pair of primers NORAD1 for the gene of interest and β-actin as housekeeping gene. For statistical analysis was used one-way ANOVA, with the condition LNA Scr 50nM for comparison. No-symbol p>0.05.

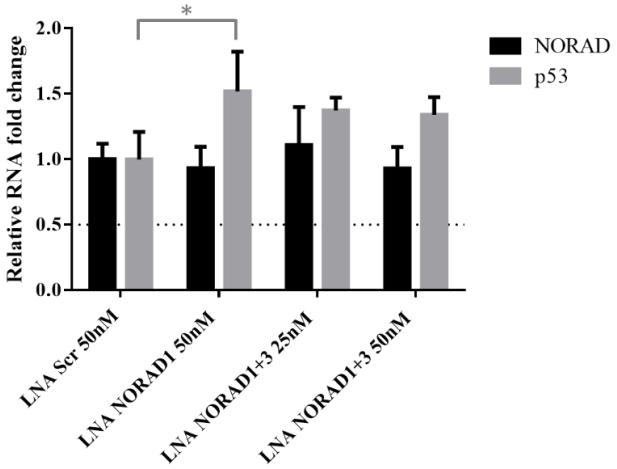

Figure 7.2: NORAD and p53 mRNA levels after NORAD knockdown, using a combination of LNA™ GapmeRs, with 24h interval between transfections. A combination of two LNA™ GapmeRs was tested, at the final concentrations of 25nM and 50nM. RT-qPCR was performed in the MDA-MB-468 cell line, using pair of primers NORAD2 for the gene of interest and β-actin as housekeeping gene. For statistical analysis was used one-way ANOVA, with the condition LNA Scr 50nM for comparison. No-symbol p>0.05, * p<0.05.

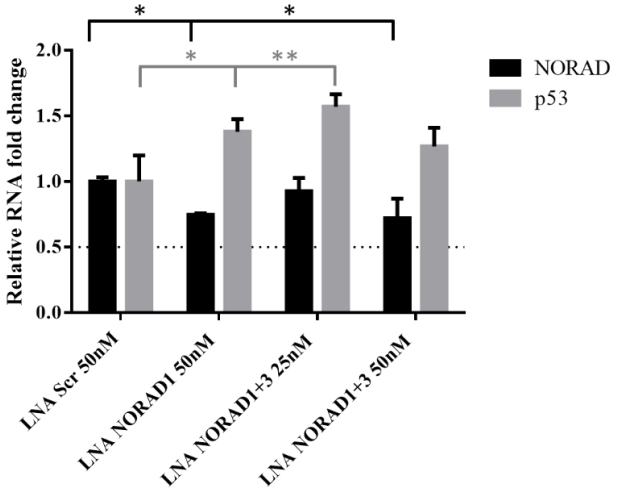

Figure 7.3: NORAD and p53 mRNA levels after NORAD knockdown, using a combination of LNA™ GapmeRs, with 48h interval between transfections. A combination of two LNA™ GapmeRs was tested, at the final concentrations of 25nM

and 50nM. RT-qPCR was performed in the MDA-MB-468 cell line, using pair of primers NORAD2 for the gene of interest and β-actin as housekeeping gene. For statistical analysis was used one-way ANOVA, with the condition LNA Scr 50nM for comparison. No-symbol p>0.05, * p<0.05, ** p<0.01.

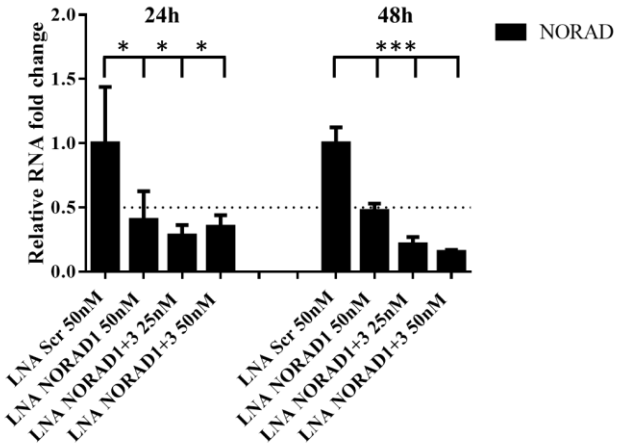

Figure 7.4: NORAD and p53 mRNA levels after NORAD knockdown, using a combination of LNA™ GapmeRs, with 24/48h interval between transfections. A combination of two LNA™ GapmeRs was tested, at the final concentrations of 25nM and 50nM. RT-qPCR was performed in the MDA-MB-468 cell line, using pair of primers NORAD2 for the gene of interest and 18S rRNA as housekeeping gene. For statistical analysis was used one-way ANOVA, with the condition LNA Scr 50nM for comparison. No-symbol p>0.05, * p<0.05 and ***p<0.001.

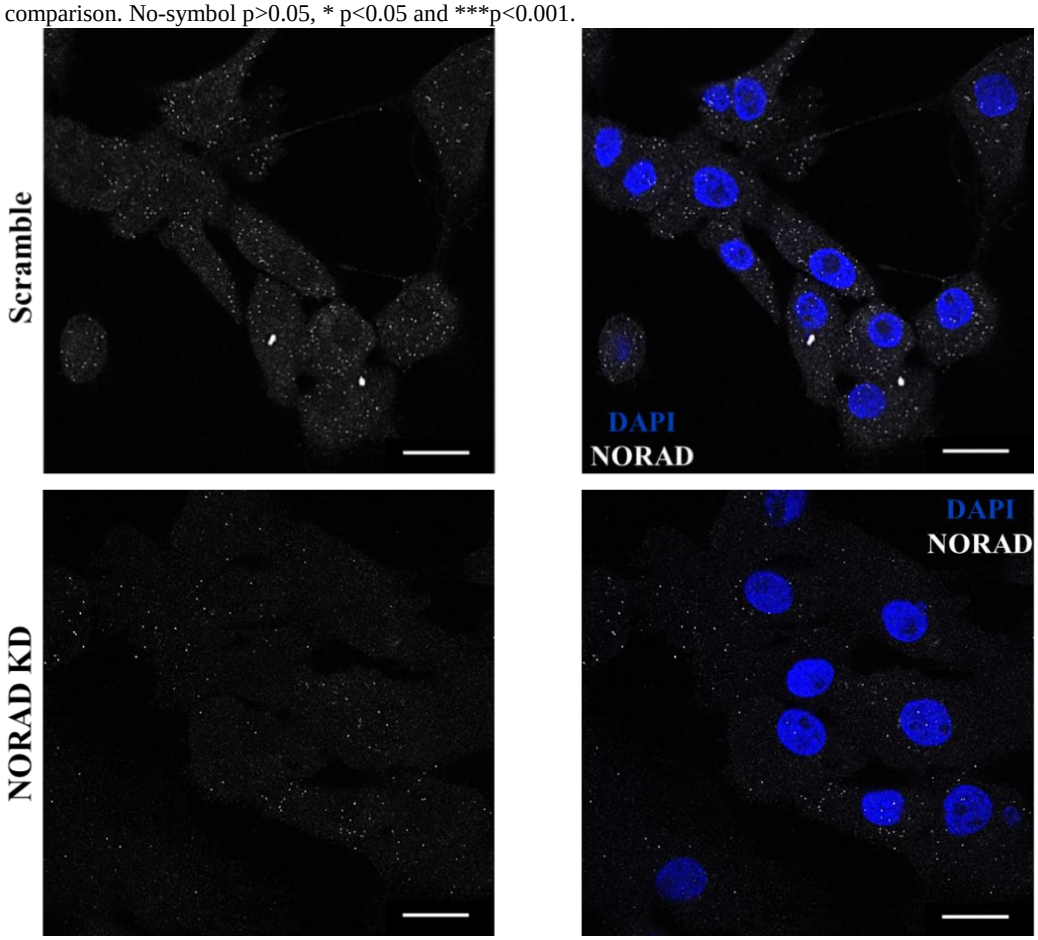

Figure 7.5: NORAD transcripts after knockdown II. smRNA FISH was performed in the MCF-10A cell line. Scale bar: 20μm.

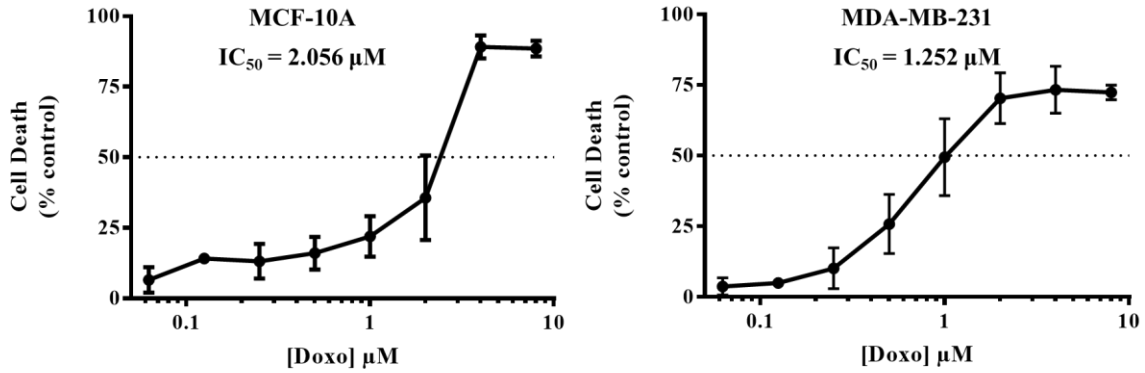

Figure 7.6: Doxorubicin IC_{50}. AlamarBlue® reduction assay was performed in MDA-MB-231 and MCF-10A cell lines. Doxorubicin IC_{50} was determined from non-linear curve fit assuming sigmoidal dose-response.